UNCLASSIFIED

AD NUMBER
AD880650
LIMITATION CHANGES
TO: **Approved for public release; distribution is unlimited.**
FROM: **Distribution authorized to U.S. Gov't. agencies and their contractors; Administrative/Operational Use; FEB 1971. Other requests shall be referred to Arnold Engineering Development Center, Arnold AFB, TN.**
AUTHORITY
AEDC ltr 16 Oct 1974

THIS PAGE IS UNCLASSIFIED

AEDC-TR-71-30

Cy 1

WAKE PROPERTIES BEHIND AN EJECTION SEAT ESCAPE SYSTEM AND AERODYNAMIC CHARACTERISTICS WITH STABILIZATION PARACHUTES AT MACH NUMBERS FROM 0.6 TO 1.5

David E. A. Reichenau

ARO, Inc.

February 1971

~~This document is subject to special export controls and each transmittal to foreign governments or foreign nationals may be made only with prior approval of Air Force Flight Dynamics Laboratory (FER), Wright-Patterson AF Base, Ohio 45433.~~

PROPULSION WIND TUNNEL FACILITY
ARNOLD ENGINEERING DEVELOPMENT CENTER
AIR FORCE SYSTEMS COMMAND
ARNOLD AIR FORCE STATION, TENNESSEE

NOTICES

WAKE PROPERTIES BEHIND AN EJECTION SEAT ESCAPE SYSTEM AND AERODYNAMIC CHARACTERISTICS WITH STABILIZATION PARACHUTES AT MACH NUMBERS FROM 0.6 TO 1.5

David E. A. Reichenau
ARO, Inc.

This document has been approved for public release its distribution is unlimited. Per AF Letter dtd 16 october, 1974 signed William O. Cole

~~This document is subject to special export controls and each transmittal to foreign governments or foreign nationals may be made only with prior approval of Air Force Flight Dynamics Laboratory (FER), Wright-Patterson AF Base, Ohio 45433.~~

FOREWORD

The work reported herein was sponsored by the Air Force Flight Dynamics Laboratory (AFFDL), Air Force Systems Command (AFSC), Wright-Patterson Air Force Base, Ohio, under Program Element 62201F, Project 1362, Task 12.

The results of the test were obtained by ARO, Inc. (a subsidiary of Sverdrup & Parcel and Associates, Inc.), contract operator of the Arnold Engineering Development Center (AEDC), AFSC, Arnold Air Force Station, Tennessee, under Contract F40600-71-C-0002. The test was conducted in the Propulsion Wind Tunnel (PWT) (16T) from September 9 to 12, 1970, and in Aerodynamic Wind Tunnel (1T) from October 13 to 14, 1970, under ARO Project No. PT0008. The manuscript was submitted for publication on December 15, 1970.

~~Information in this report is embargoed under the Department of State International Traffic in Arms Regulations. This report may be released to foreign governments by departments or agencies of the U. S. Government subject to approval of the Air Force Flight Dynamics Laboratory (FER), or higher authority within the Department of the Air Force. Private individuals or firms require a Department of State export license.~~

This technical report has been reviewed and is approved.

George F. Garey
Lt Colonel, USAF
AF Representative, PWT
Directorate of Test

Joseph R. Henry
Colonel, USAF
Director of Test

ABSTRACT

A test was conducted in the Propulsion Wind Tunnel (16T) of the Propulsion Wind Tunnel Facility to determine the flow field in the wake of an ejection seat escape system at transonic flight conditions, and to determine the performance characteristics of a stabilization parachute attached to the back of the ejection seat model. The results were obtained for both simulated rocket-off and rocket-on conditions through a model angle-of-attack range from 0 to 30 deg. High pressure air was used to simulate the escape rocket jet plume at a sea-level altitude. The results show that the ejection seat model was statically unstable, but became longitudinally stable with the parachute for the test range investigated.

CONTENTS

APPENDIX
ILLUSTRATIONS

NOMENCLATURE

b	Model reference length, 2.0 ft
C_A	Model axial-force coefficient, $F_A/q_\infty S$
C_{D_o}	Parachute drag coefficient, $D_p/q_\infty S_o$
C_m	Model pitching-moment coefficient, $M_m/q_\infty Sb$
C_N	Model normal-force coefficient, $F_N/q_\infty S$
D	Model reference width, 1.025 ft

D_c	Constructed diameter of guide surface parachute, 2.25 ft
D_p	Parachute drag force, lb
F_A	Model axial force, lb
F_N	Model normal force, lb
F_Y	Side force, lb
ℓ	Suspension line length, in.
M_ℓ	Rolling moment, ft-lb
M_m	Model pitching moment, ft-lb
M_n	Yawing moment, ft-lb
M_w	Wake local Mach number
M_∞	Free-stream Mach number
p_c	Nozzle total pressure (chamber pressure), psfa
p_∞	Free-stream static pressure, psfa
q_w	Wake local dynamic pressure, psf
q_∞	Free-stream dynamic pressure, psf
S	Model reference area, 1.73 sq ft
S_o	Parachute reference area Hemisflo (based on nominal diameter), 4.906 sq ft Guide Surface (based on design diameter), 3.974 sq ft
X	Axial location of rake probe or parachute downstream of the model center-of-gravity location, positive downstream, ft
Y	Horizontal location of rake probe from the model center-of-gravity location, positive to the right looking upstream, ft
Z	Vertical location of rake probe from the model center-of-gravity location, positive up looking upstream
α	Model angle of attack, deg

θ_N Nozzle semidivergence angle, deg

ψ Angle of yaw, deg

NOTE: The force and moment coefficients are in the body-axis system (Fig. 9).

SECTION I
INTRODUCTION

The purpose of this test program was to determine the flow field in the wake of an ejection seat with an attached dummy crew member during simulated rocket-off and rocket-on conditions and to determine the performance characteristics of a stabilization parachute attached to the ejection seat model. The wake was surveyed with a pressure rake at horizontal positions from 5.8 to 9.7 body widths aft of the model center of gravity and vertically from 2.4 body widths above to 2.4 body widths below the model center of gravity. The stabilization parachutes were attached to the back of the ejection seat model with various riser lengths to investigate parachute performance at various trailing distances.

The data in this report represent typical results obtained during the investigation. The data were obtained during simulated rocket-off and rocket-on conditions at Mach numbers from 0.6 to 1.5 for model angles of attack from 0 to 30 deg. High pressure air was used to simulate the escape rocket jet plume at sea-level altitude. Previous tests showing the basic ejection seat aerodynamic characteristics, and the aerodynamic interference effects of the simulated catapult rocket plume on the ejection seat aerodynamic characteristics are presented in Ref. 1.

SECTION II
APPARATUS

2.1 TEST FACILITY

The Propulsion Wind Tunnel (16T) is a closed-circuit, continuous flow wind tunnel capable of being operated at Mach numbers from 0.20 to 1.60. The test section is 16 by 16 ft in cross section and 40 ft long. The tunnel can be operated within a stagnation pressure range from 120 to 4,000 psfa, depending on the Mach number. Stagnation temperature can be varied from an average minimum of about 80 to a maximum of 160°F. Perforated walls in the test section allow continuous operation through the Mach number range with a minimum of wall interference.

Details of the test section, showing the model location and support system arrangement, are presented in Fig. 1 (Appendix). A wind-tunnel installation photograph, showing the model with both the survey rake support system and the decelerator in Tunnel 16T, is presented in Fig. 2. A more extensive description of the tunnel and its operating characteristics is contained in the Test Facilities Handbook, Ref. 2.

2.2 TEST ARTICLE

The model tested consisted of a 0.5-scale representation of an ejection seat escape system occupied by a dummy crew member of average size in normal flying clothes and equipment. The model had a frontal area of 1.73 sq ft and a side area of 1.71 sq ft. Major dimensions of the model are presented in Fig. 3. The escape rocket was positioned in the lower aft portion of the seat and was attached to the sting so that the model was isolated from the jet reaction force.

The crew member was constructed of cloth impregnated with phenolic resin and was rigidly attached to the metal seat housing a six-component balance. The arms of the crew member simulated an ejection position holding the ejection handle control on the arm rests. The nozzle configuration used simulated the plume shape of a full-scale 2174-518 rocket catapult at sea-level altitude. The fixed-area-ratio nozzle was designed so that the initial turning angle of the jet plume simulated the initial turning angle of the 2174-518 rocket plume at sea level altitude, Ref. 3. Details of the nozzle are given in Fig. 4. High pressure air, supplied to the nozzle through the center of the sting support system, was controlled remotely over a chamber pressure range from 0 to 1800 psia. A hydraulic actuator was used to provide remote variation of model angle of attack through the range of 0 to 30 deg.

The model wake was surveyed with and without rocket plume simulation with a pressure rake containing thirteen cone probes, each cone instrumented with a pitot and four static orifices. The static orifices were manifolded together to give one average pressure. The sting-mounted rake was remotely translated horizontally from 5.8 to 9.7 body widths aft of the model center of gravity and translated vertically 2.4 body widths above and below the model center of gravity. The pressure rake details are shown in Fig. 5.

The stabilization parachute assembly is shown in Fig. 6. The parachute riser line was affixed to the back of the ejection seat at four points by a bridle-load link combination. A strain-gage load link was placed in each of the four bridle legs, and a load link, measuring the total parachute drag, was placed between the riser line and the bridle assembly.

The two types of stabilization parachutes investigated were the Hemisflo and the Guide Surface parachute. The Hemisflo parachute was constructed of 0.75-in. nylon ribbons and the Guide Surface parachute was constructed of a relatively nonporous nylon cloth. The bridle, riser, and suspension lines of both types of parachutes were also of nylon construction. A dimensioned sketch of the two types of stabilization parachutes is presented in Figs. 7 and 8. The Hemisflo parachute had a nominal diameter of 2.50 ft and a geometric porosity of 15 percent. The Guide Surface had a constructed diameter of 2.25 ft.

2.3 INSTRUMENTATION

An internally mounted, six-component, strain-gage balance was used to measure the model forces and moments. Four strain-gage load links were used to measure the parachute drag loads exerted on each bridle leg at the model attachment points, and a fifth load link was used to measure the total parachute drag between the bridle and riser line. The jet chamber pressure and temperature were measured with a 0- to 2500-psi gage transducer and a copper-constantan thermocouple, respectively. The pressure rake consisted of 13 conical probes, each instrumented with a pitot and four static orifices. The static orifices were interconnected to give one average pressure. The vertical and axial location of the pressure rake was determined by linear potentiometers.

The electrical output signals from the balance, load links, pressure transducers, thermocouple, and potentiometers were transmitted through analog-to-digital converters to a Raytheon 520 computer for final data reduction while the test was in progress. Also, the balance and load link outputs were continuously recorded on direct-writing oscillographs for monitoring model dynamics and parachute drag. Five motion-picture cameras and a television camera were used to document and monitor the test.

SECTION III
TEST DESCRIPTION

3.1 GENERAL

After the prescribed tunnel conditions were established during the wake survey phase, jet-off and jet-on data were obtained while holding the Mach number constant and varying the model angle of attack. At each model angle of attack, the wake was surveyed from 5.8 to 9.7 body widths aft of the model center of gravity and vertically from 2.4 body widths above to 2.4 body widths below the model center of gravity.

For the ejection seat and parachute portion of testing, the parachute deployment was obtained by permitting the parachute to hang freely from the ejection seat model and to deploy as tunnel conditions were achieved. Different riser lengths were used to obtain data at the various axial locations. The parachute steady-state loads were calculated by averaging the analog output from the load links and balance over 1-sec intervals. Motion pictures and steady-state data were obtained at various axial locations downstream of the model at various model angles of attack.

For the jet-on data, a continuous supply of high pressure air was ducted to the model for rocket simulation. The nozzle design and jet pressure used during these tests simulated the full-scale rocket shape at a sea-level altitude. (It should be mentioned that the full-scale rocket catapult operates at a constant chamber pressure of 4,000 psia, but in order not to exceed the load limit of the balance over the Mach number range, it was necessary to vary both the jet chamber and the free-stream static pressure and yet maintain a constant ratio (p_c/p_∞). The jet chamber pressure was varied from 450 psia at $M_\infty = 0.6$ to 1800 psia at $M_\infty = 1.5$.

The ejection seat model was tested at free-stream Mach numbers from 0.6 to 1.5 through a model pitch range from 0 to 30 deg. The dynamic pressure was varied from 170 to 690 psf, and the Reynolds number per foot was varied from 0.67 to 10^6 to 2.2×10^6.

3.2 DATA REDUCTION

The model force and moment data obtained during this test were corrected for weight tares and reduced to coefficient form in the body-axis system as shown in Fig. 9. The moment coefficients are referred to the model reference center-of-gravity position shown in Fig. 3. All model force and moment coefficients are based on the seat height of 2 ft and projected model frontal area of 1.73 sq ft. The force and moment coefficients do not include the jet reaction force.

3.3 PRECISION OF MEASUREMENTS

An estimate of the accuracy of measurements is presented below.

M_∞	$\pm M_\infty$	$\pm\alpha$	$\pm C_A$	$\pm C_N$	$\pm C_m$	$\pm C_{D_o}$	$\pm q_w$	$\pm M_w$
0.6	0.005	0.1	0.008	0.05	0.008	0.020	7 psf	0.024
1.5	0.016	0.1	0.003	0.02	0.003	0.022	10 psf	0.035

SECTION IV
RESULTS AND DISCUSSION

This investigation was conducted for the purpose of determining the flow field in the wake of an ejection seat escape system and of determining the performance characteristics of a stabilization parachute attached to the ejection seat model. The results were obtained for both simulated rocket-off and rocket-on conditions through a model angle-of-attack range from 0 to 30 deg. High pressure air was used to simulate the escape rocket jet plume at a sea-level altitude.

The data in this report represent typical results obtained during the investigation. The complete test data were forwarded to AFFDL for final analysis.

4.1 MODEL WAKE PROPERTIES

Presented in Figs. 10 through 15 are the local wake properties in the form of the ratio of the local Mach number to free-stream Mach number and local wake dynamic pressure to free-stream dynamic pressure. The local wake Mach number ratios (M_w/M_∞) for both jet-off and jet-on conditions are presented in Figs. 10 and 11 at various X/D locations with the ejection seat model at α = 0 deg. The wake was investigated from Z/D = -2.4 to 2.4 at each condition, and the model vertical location at α = 0 was between Z/D = -1.4 and 1.4. In general, the effect of the jet plume at M_∞ = 0.60 was to increase the local Mach number of the flow field at all X/D locations. At M_∞ = 1.5, the effect of the jet plume on the local wake Mach number was less pronounced and generally reduced the wake Mach number in the flow field region influenced by the jet plume (-2.4 < Z/D < 0). The wake caused by the sting support system was apparent in the region below the model (-2.4 < Z/D < 1.4).

The effects of varying the model angle of attack on the local wake Mach number distribution are presented in Fig. 12 for jet-off conditions. Increasing the model angle of attack produced a significant change in the local wake Mach number at various Z/D locations.

Representative flow field data are presented in Figs. 13 and 14 showing the local dynamic pressure distribution at various X/D locations for jet-off and jet-on conditions. Comparing the data in Figs. 13a and 14a for jet-off conditions, it may be seen that increasing the X/D location increased the local dynamic pressure level and reduced the gradients at M_∞ = 0.60 and 1.50. In general, the trends were the same for the jet-on conditions (Figs. 13b and 14b) with the exception of the $M_\infty = 0.6$ results, where the local dynamic pressure level decreased with increasing X/D locations in the flow field region influenced by the jet plume.

From the comparison of jet-off and jet-on data in Figs. 13 and 14, it may be seen that the simulated jet at $M_\infty = 0.6$ increased the local dynamic pressure level over the entire flow field at the various X/D locations. However, at $M_\infty = 1.5$, the simulated jet increased the local dynamic pressure level only in the flow field region influenced by the jet plume. In general, there was little difference in the local dynamic pressure gradients near the model ($-1.4 < Z/D < 1.4$) as a result of the jet simulation.

Figure 15 shows the effect of increasing the model angle of attack on the local dynamic pressure distribution at an X/D location of 5.8 with the jet off. Generally, the level of the local dynamic pressure increased with increasing model angle of attack in the flow field affected by the model. Also, the interference effects caused by the model support system appear to have influenced a larger portion of the flow field at the higher angles of attack.

4.2 PARACHUTE CHARACTERISTICS

A Hemisphere and a Guide Surface parachute were investigated as a stabilization device for the ejection seat model. Since only a limited amount of data were obtained with the Guide Surface parachute, no comparative data will be presented. The measured drag coefficient of the Guide Surface parachute (based on a constructed diameter of 2.25 ft) was 0.42 and 0.43 at $M_\infty = 0.60$ and 0.90, respectively, with the model at zero angle of attack. Visual analysis of television monitors and motion pictures showed that the Hemisflo and Guide Surface parachutes exhibited full canopy inflation at all test conditions.

Various riser line lengths were used between the Hemisflo parachute and the ejection seat. The effect of the parachute trail distance, X/D, on the parachute drag coefficient, C_{D_0}, is presented in Fig. 16. The effect of jet simulation on the parachute drag coefficient is also shown for comparative purposes. The data show that at a given free-stream Mach number, the parachute drag coefficient increased with increasing X/D locations with the greatest increase occurring at the lower Mach numbers. The increase in drag coefficient was primarily caused by the ejection seat wake becoming less prominent as the X/D location was increased. Analysis of motion pictures shows that the parachute oscillatory motions decreased as the X/D locations increased. However, in the actual case, a smaller trail distance is desirable since it minimizes the effect of the aircraft horizontal stabilizer interference on the aircraft. Photographs of the Hemisflo parachute, at various trail distances and model angles of attack, are presented in Fig. 17 for a jet-off condition.

The effect of jet simulation on the parachute drag coefficient may also be seen in Fig. 16. The data obtained with the model at $\alpha = 0$ deg show that the jet air increased the parachute drag coefficient at each test condition. Motion-picture coverage obtained during jet simulation showed that the jet wake had essentially no effect on dynamics or trailing angle of the Hemisflo parachute. The Guide Surface parachute, which exhibited more erratic dynamics than the Hemisflo parachute, moved toward the jet wake during jet simulation. Photographs of the Guide Surface parachute at various model angles of attack, showing the effect of jet simulation, are presented in Fig. 18.

The effect of the ejection seat angle of attack on the Hemisflo drag coefficient is shown in Fig. 19 for jet-off and jet-on conditions. Generally, the parachute drag coefficient increased with increasing angle of attack at each X/D location. However, some adverse effects on the parachute drag occurred at the high angles of attack, particularly for the jet-off conditions.

4.3 AERODYNAMIC CHARACTERISTICS

The shape of an ejection seat must conform to airplane geometric constraints that inevitably produce an aerodynamically unstable seat. The basic aerodynamic characteristics and aerodynamic interference effects of rocket jet simulation on the ejection seat without a stabilization parachute are shown in Ref. 1. Some typical results are presented in Figs. 20 and 21 showing the effect of a parachute as a retardation and stabilization device. The Hemisflo parachute increased the ejection seat axial-force coefficient for all test conditions as shown in Fig. 20. The static longitudinal stability characteristics of the ejection seat model, with and without the stabilization parachute, can be interpreted from the slope of the pitching-moment versus axial-force coefficient plots presented in Fig. 21. The ejection seat model without the stabilization parachute was unstable at all test conditions for the range of angle of attack investigated. The ejection seat model with the stabilization parachute was stable at all test conditions with stable trim points occurring at approximately $\alpha = 13$ deg at $M_\infty = 0.60$ to $\alpha = 6$ deg at $M_\infty = 1.50$ for the jet-off condition. The jet simulation had little effect on the static stability characteristics.

SECTION V
CONCLUDING REMARKS

Tests were conducted to determine the flow field in the wake of an ejection seat escape system at transonic flight conditions and to determine the performance characteristics of a stabilization parachute attached to the ejection seat model during rocket-off and simulated rocket-on conditions. The following observations are a result of these tests:

1. The level of the local Mach number and dynamic pressure increased, and the gradients were decreased as X/D increased.

2. The effect of jet simulation was to increase the level of the local Mach number and dynamic pressure at $M_\infty = 0.60$.

3. The stabilization parachute drag coefficients increased with increasing trail distances at each test condition.

4. The stabilization parachute exhibited full canopy inflation throughout the Mach number range of the investigation.

5. The ejection seat model was statically unstable but became longitudinally stable with the parachute for the test range investigated.

REFERENCES

1. Reichenau, David E. A. "Aerodynamic Characteristics of an Ejection Seat Escape System with Cold Flow Rocket Plume Simulation at Mach Numbers from 0.6 to 1.5" AEDC-TR-69-218 (AD860482), October 1969.

2. Test Facilities Handbook (Eighth Edition) "Propulsion Wind Tunnel Facility, Vol. 5." Arnold Engineering Development Center, December 1969 (AD863646).

3. Pindzola, M. "Boundary Simulation Parameters for Underexpanded Jets in a Quiescent Atmosphere." AEDC-TR-65-6 (AD454770), January 1965.

APPENDIX
ILLUSTRATIONS

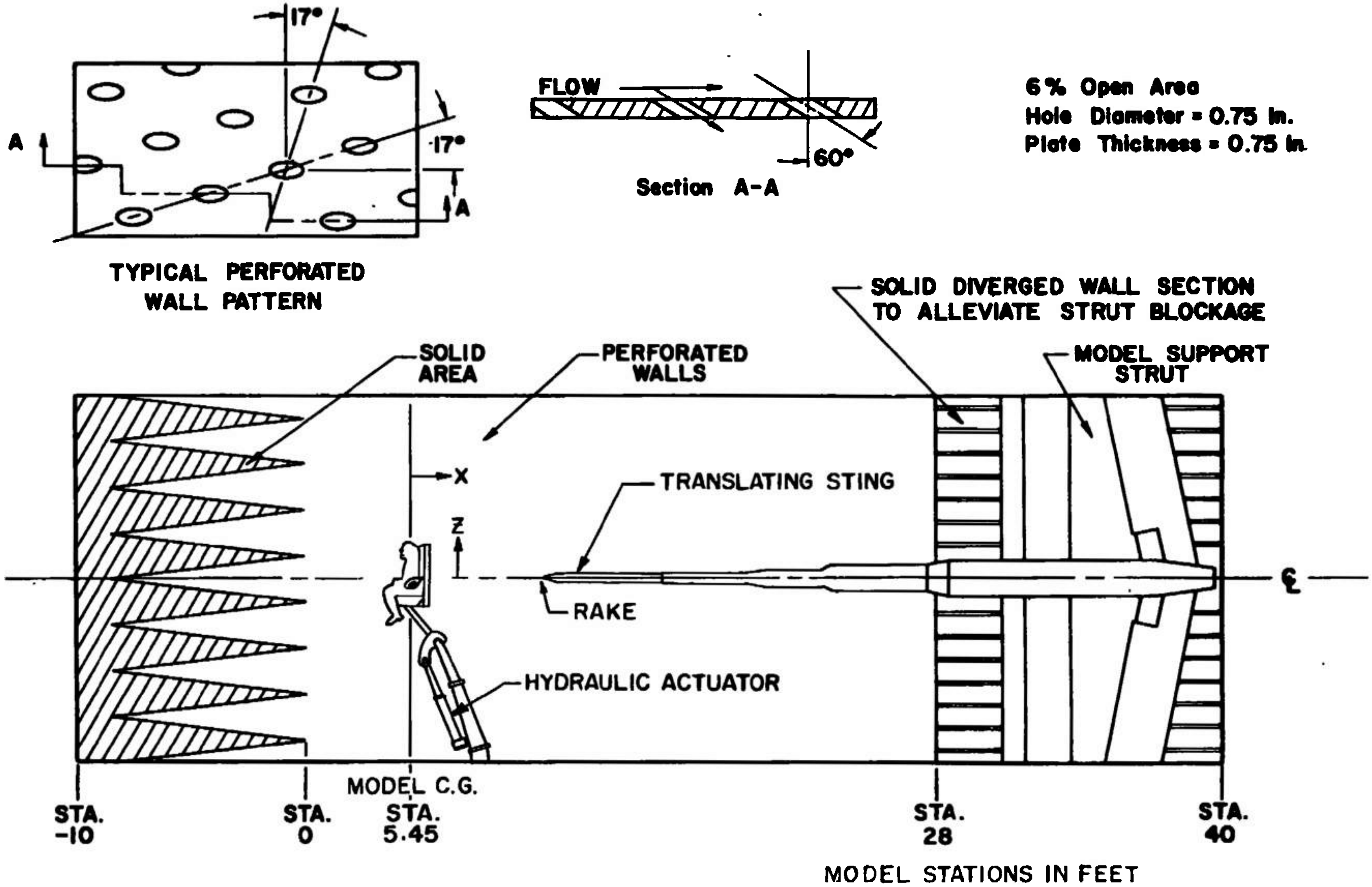

Fig. 1 Location of Model in Test Section

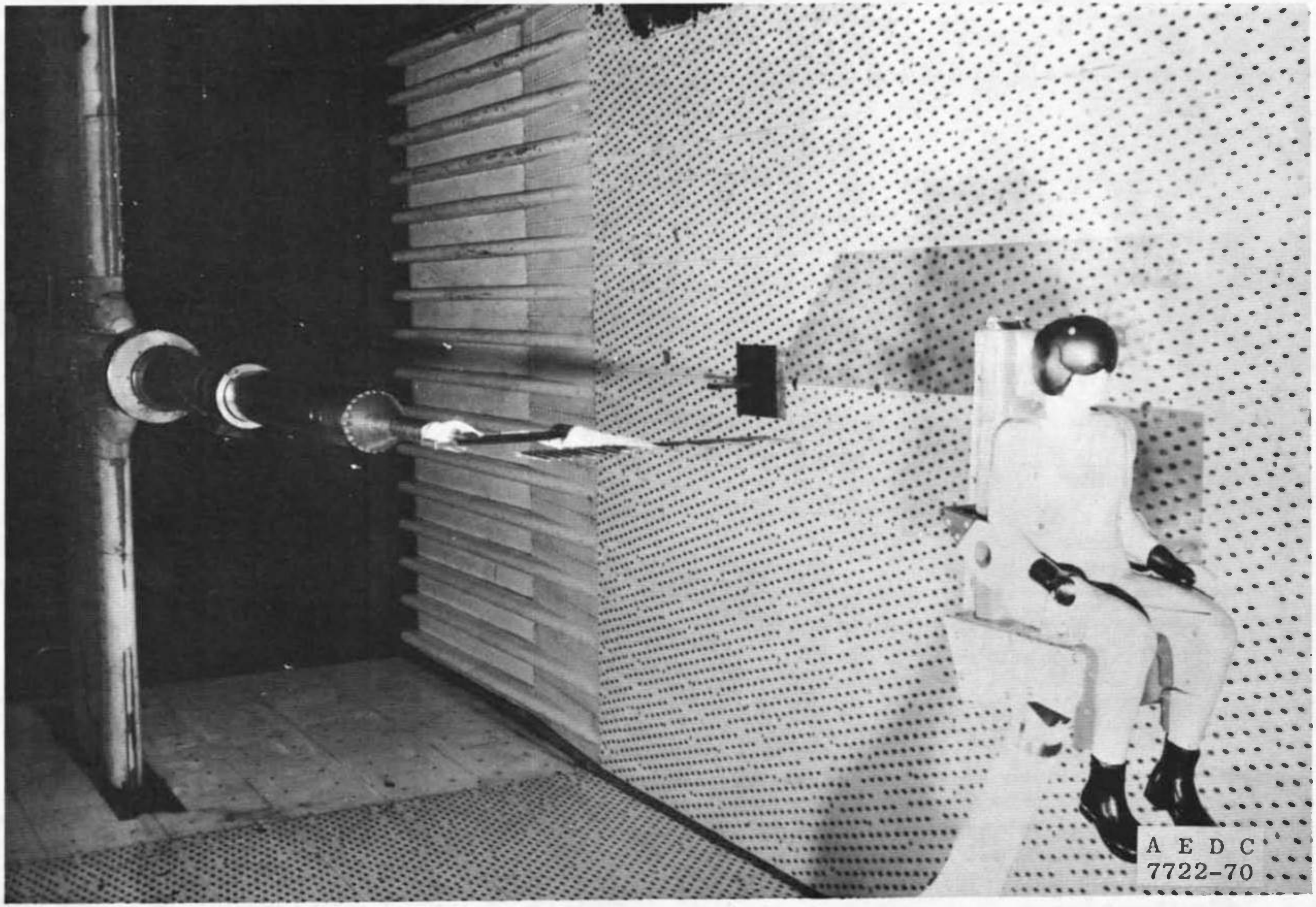

a. Wake Survey Phase
Fig. 2 Installation Photographs

b. Parachute Phase
Fig. 2 Concluded

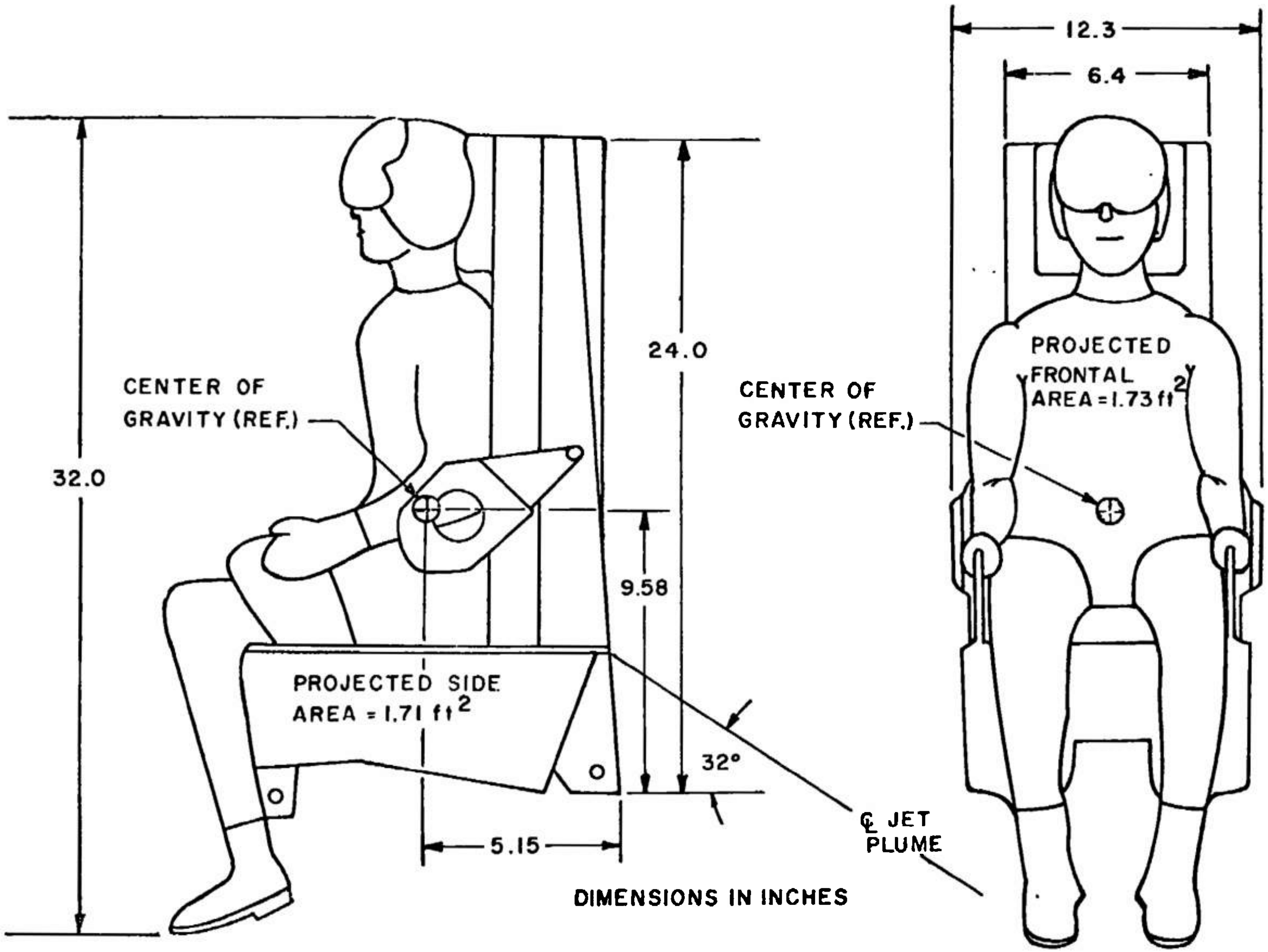

Fig. 3 Major Dimensions of the Model

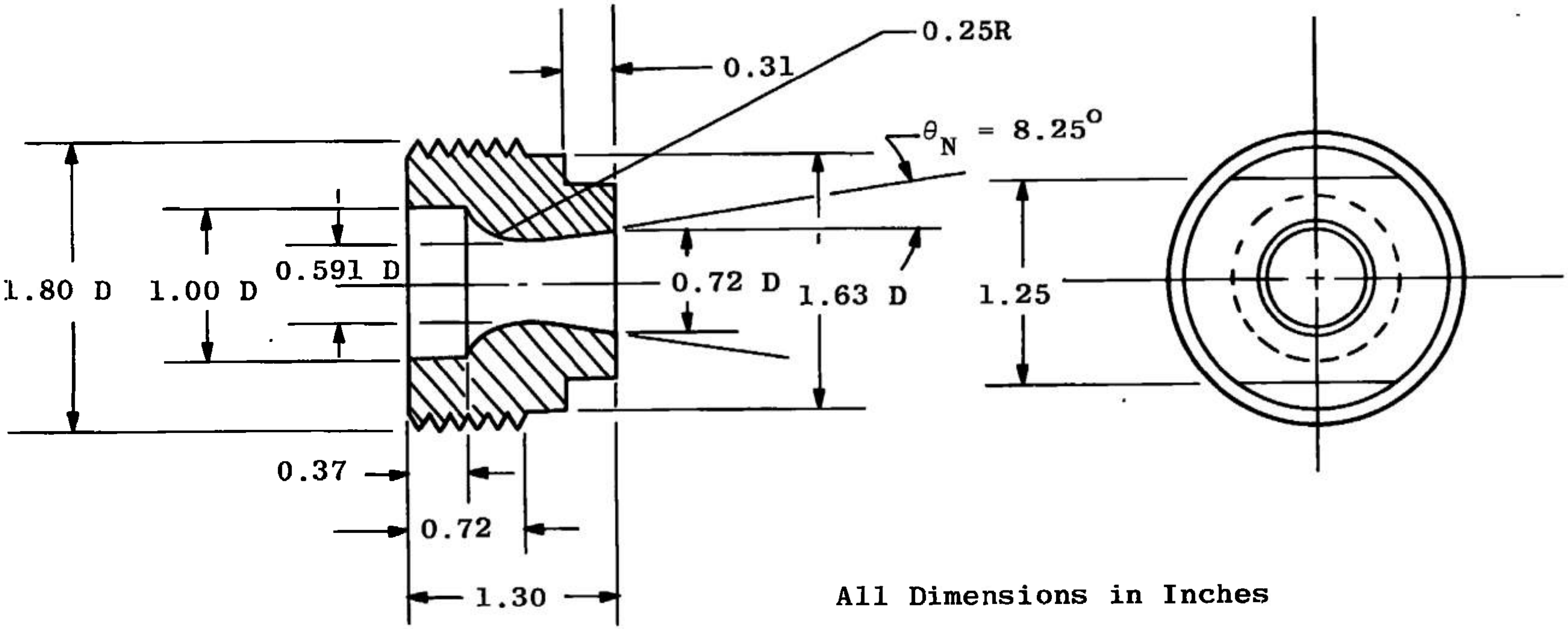

Fig. 4 Nozzle Details

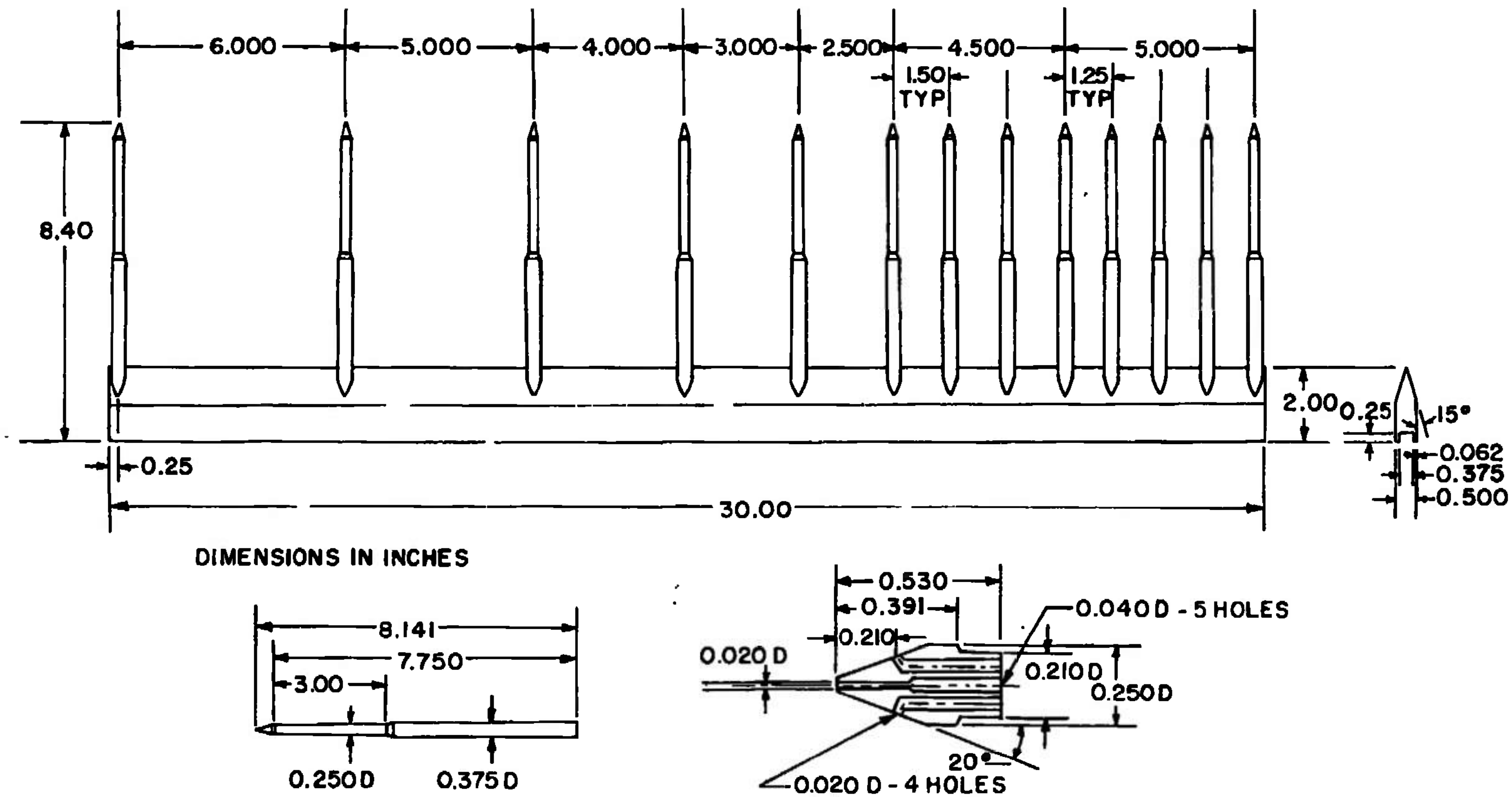

Fig. 5 Rake Probe Details

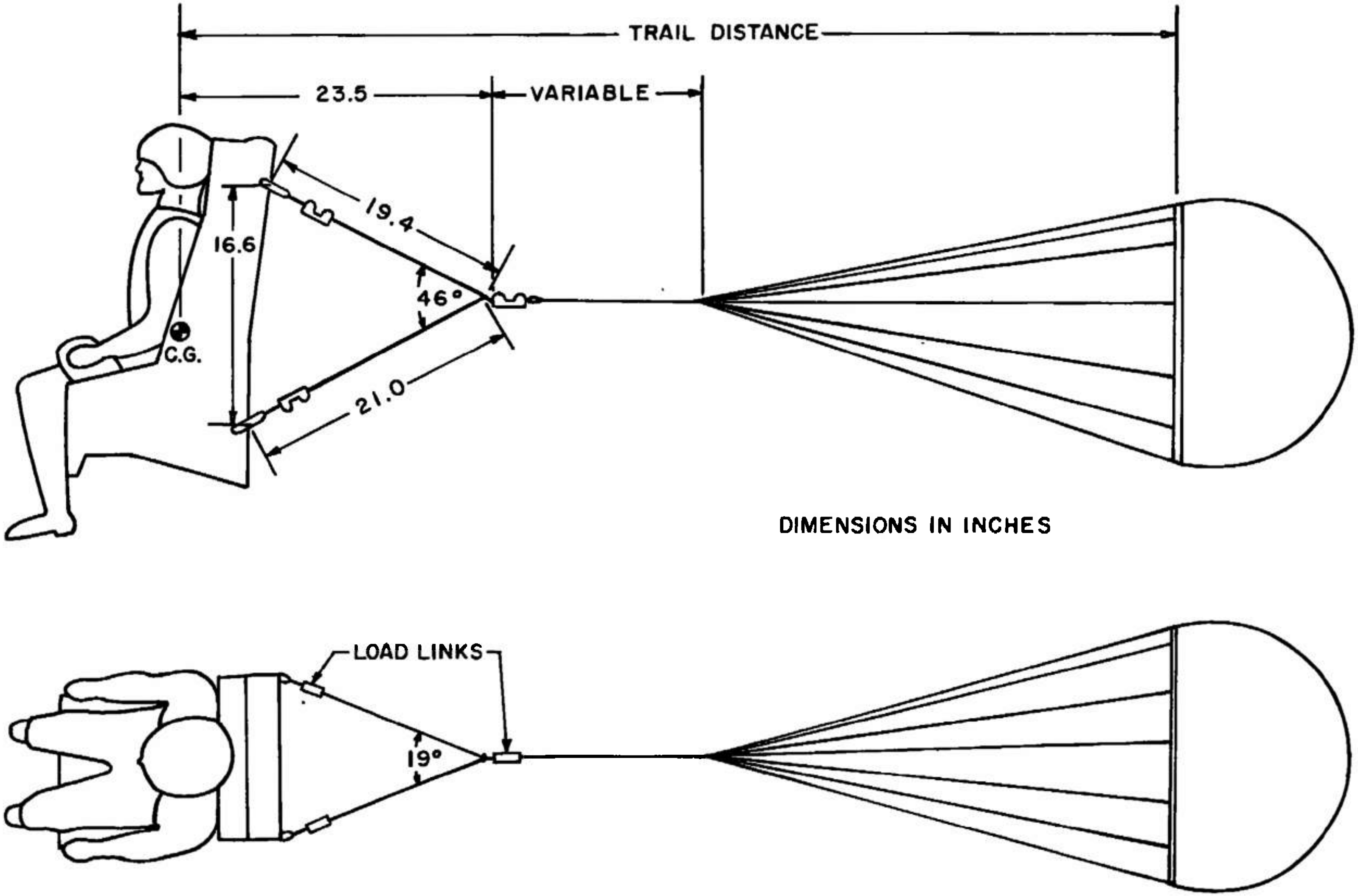

Fig. 6 General Drawing of Parachute Assembly

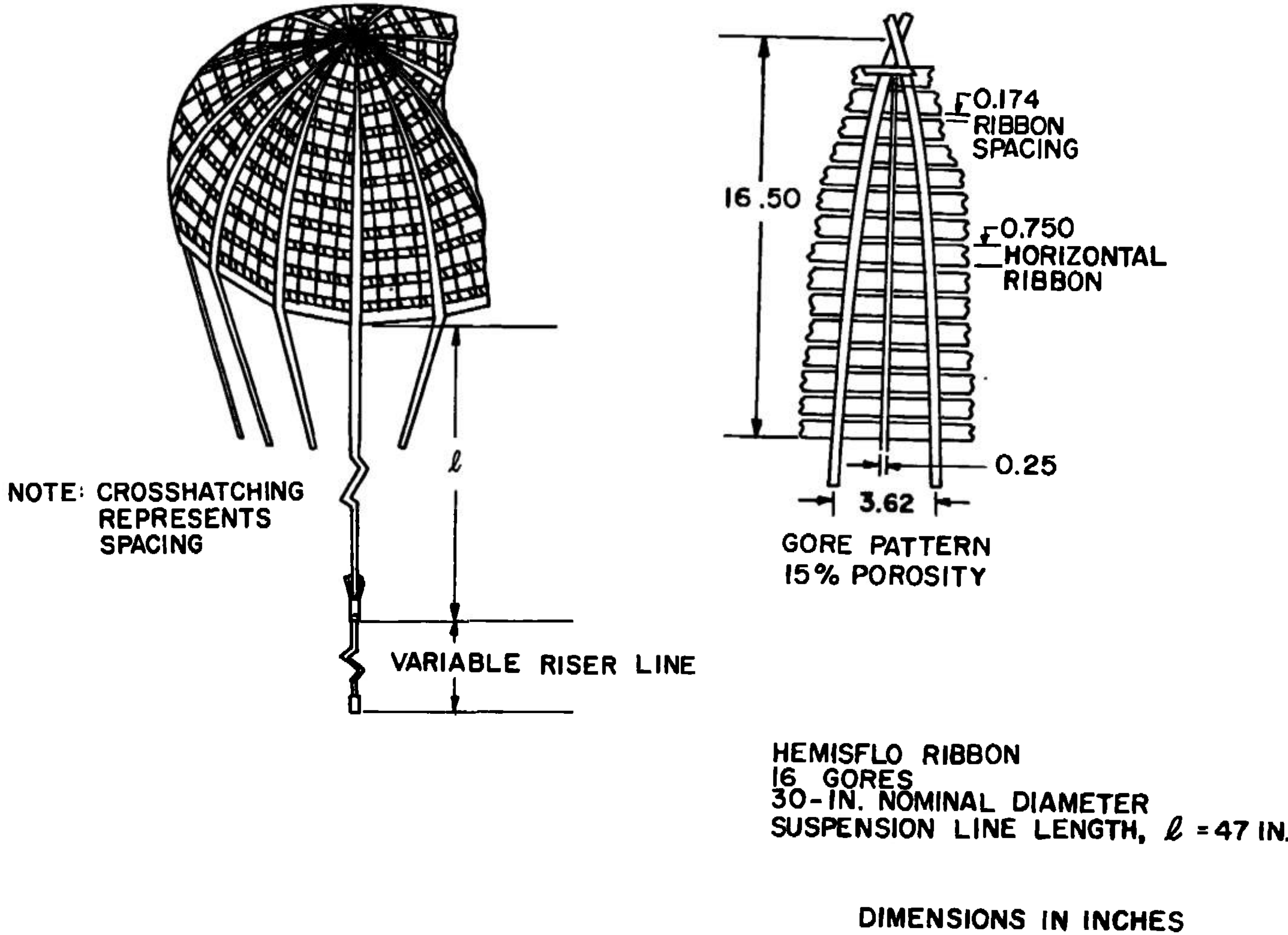

Fig. 7 Dimensioned Sketch of the Hemisflo Parachute

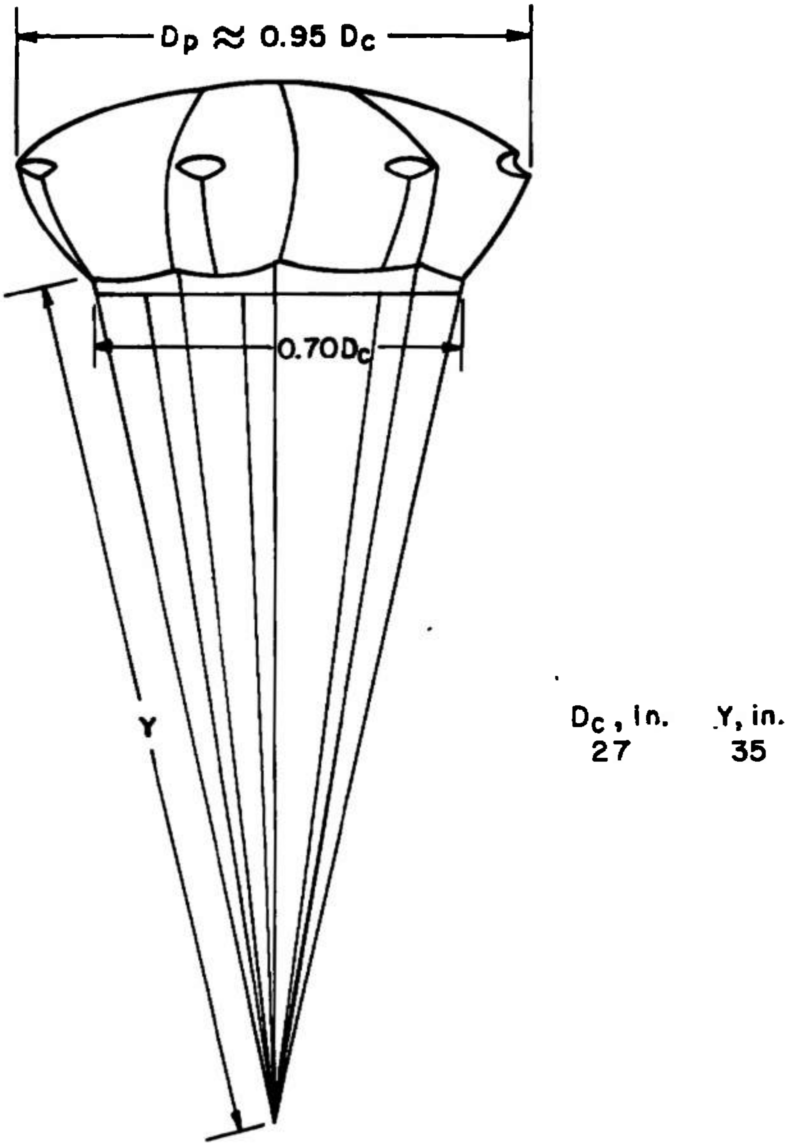

Fig. 8 Dimensioned Sketch of the Guide Surface Parachute

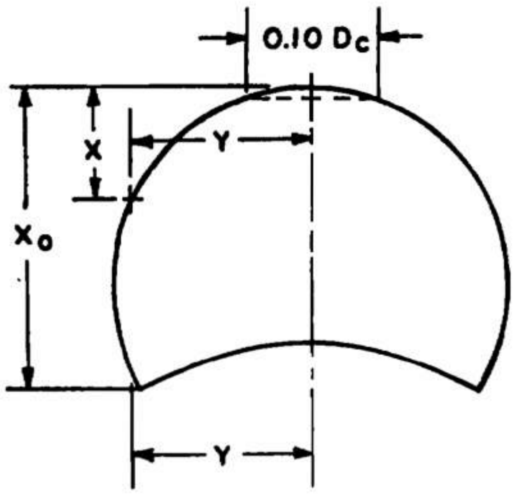

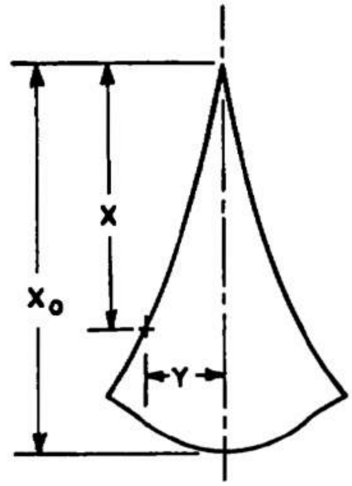

GUIDE SURFACE COORDINATES

X/X_0	Y/X
0.050	5.520
0.100	3.810
0.150	2.960
0.200	2.430
0.300	1.800
0.400	1.420
0.500	1.170
0.600	0.977
0.700	0.823
0.800	0.705
0.900	0.603
0.919	0.586
0.919	0.000
0.950	0.559
0.950	0.305
1.000	0.517

$X_0 = 0.230\ D_c$

ROOF COORDINATES

X/X_0	Y/X
0.100	0.532
0.150	0.520
0.200	0.516
0.300	0.514
0.400	0.511
0.500	0.511
0.600	0.509
0.700	0.525
0.800	0.588
0.866	0.713
0.900	0.496
0.950	0.261
0.975	0.1625
1.000	0.000

$X_0 = 0.500\ D_c$

DIMENSIONS IN INCHES

Fig. 8 Concluded

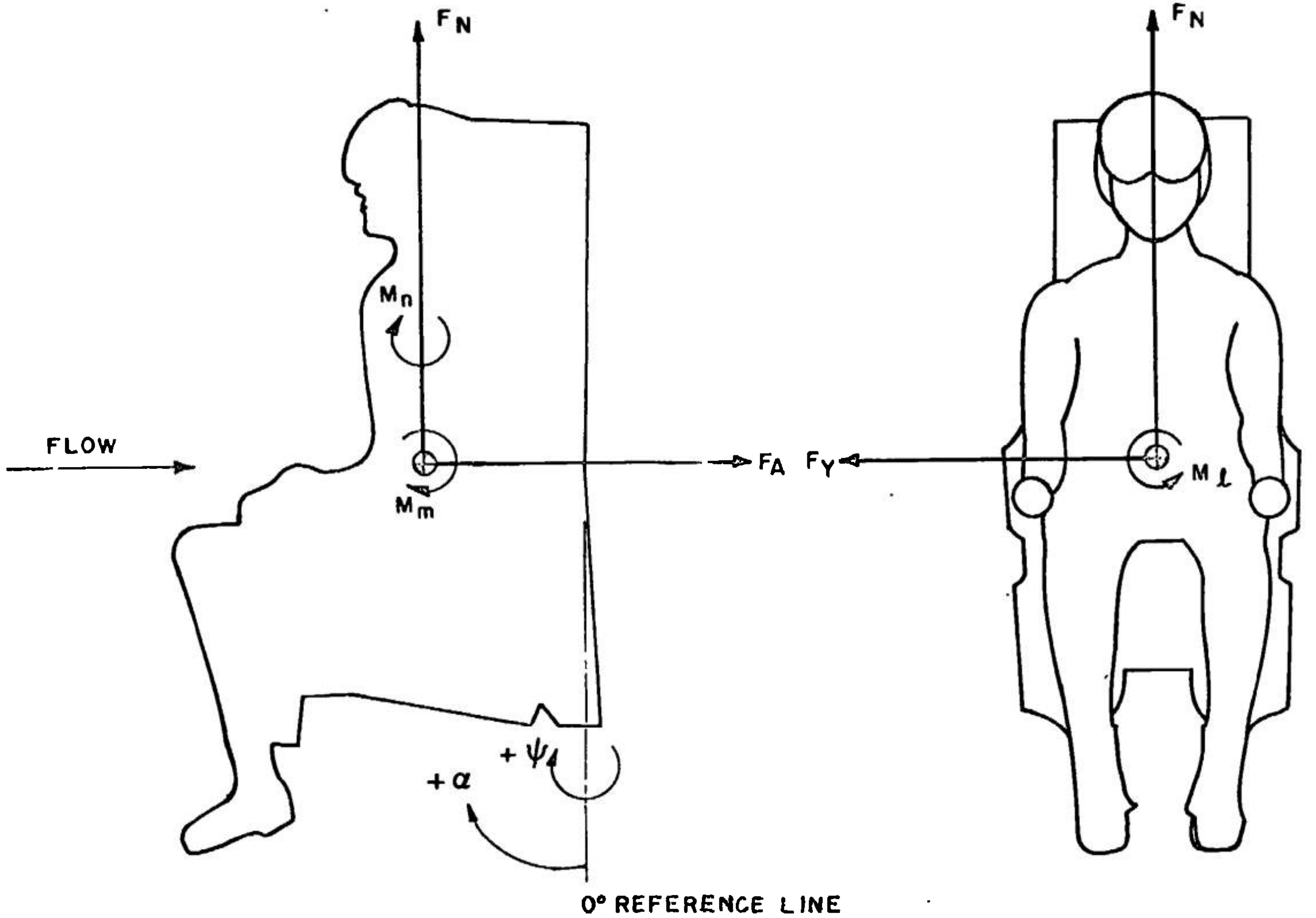

NOTE: MODEL AT 0° ANGLE OF ATTACK

Fig. 9 Body-Axis Reference System

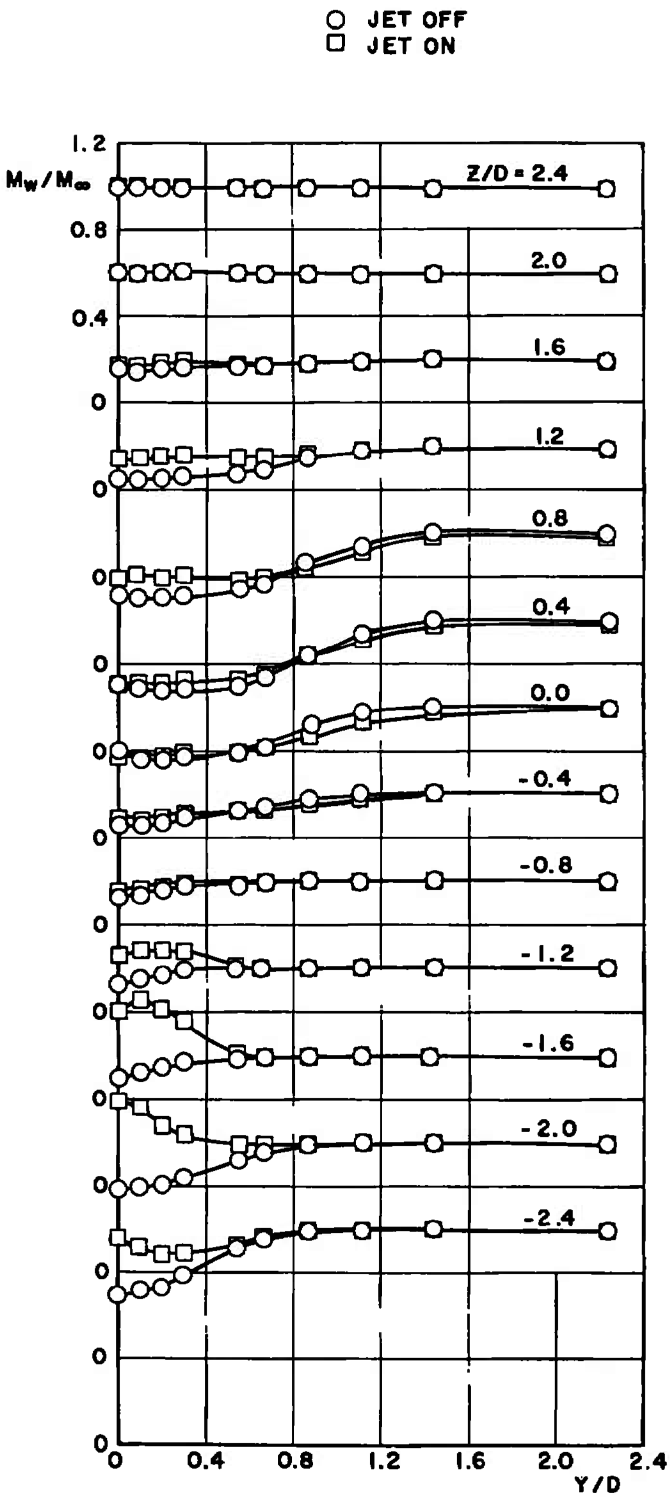

a. X/D = 5.8

Fig. 10 Local Mach Number Variation for Jet-Off and Jet-On Conditions, M_∞ = 0.60, α = 0 deg

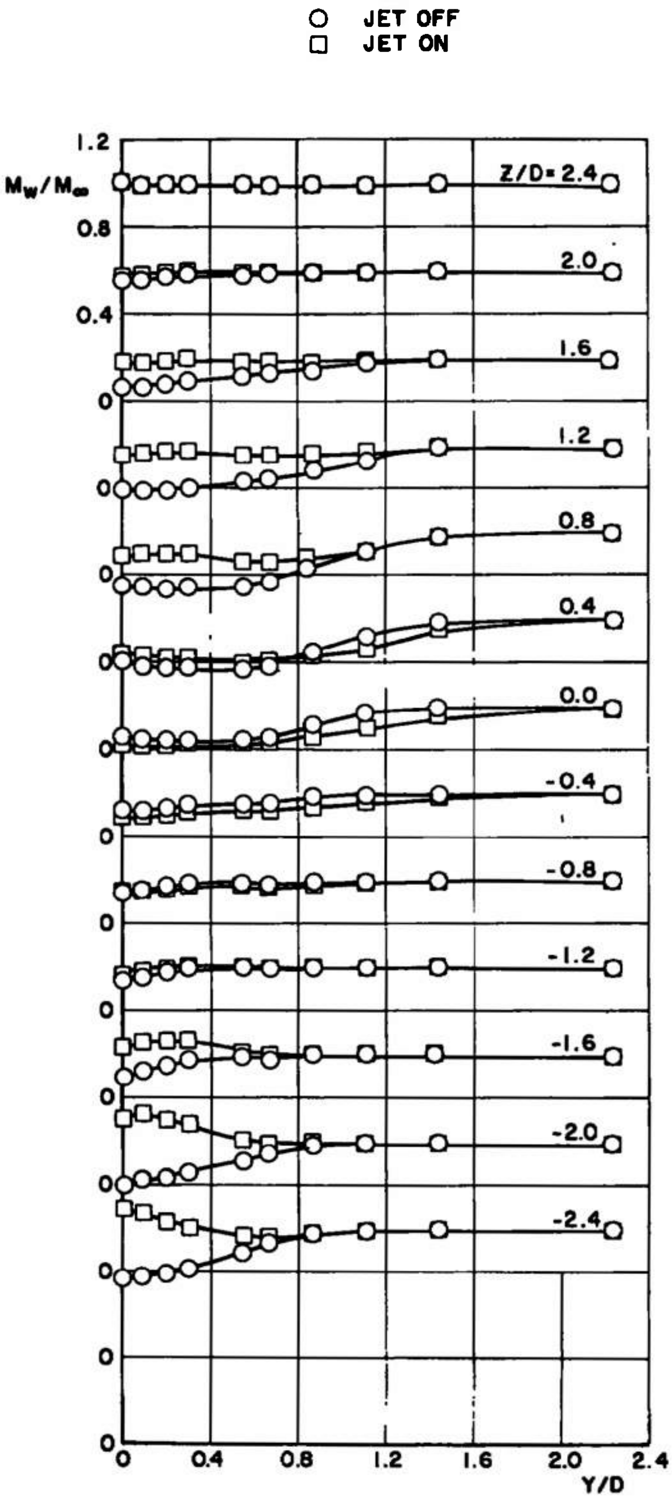

b. X/D = 7.8
Fig. 10 Continued

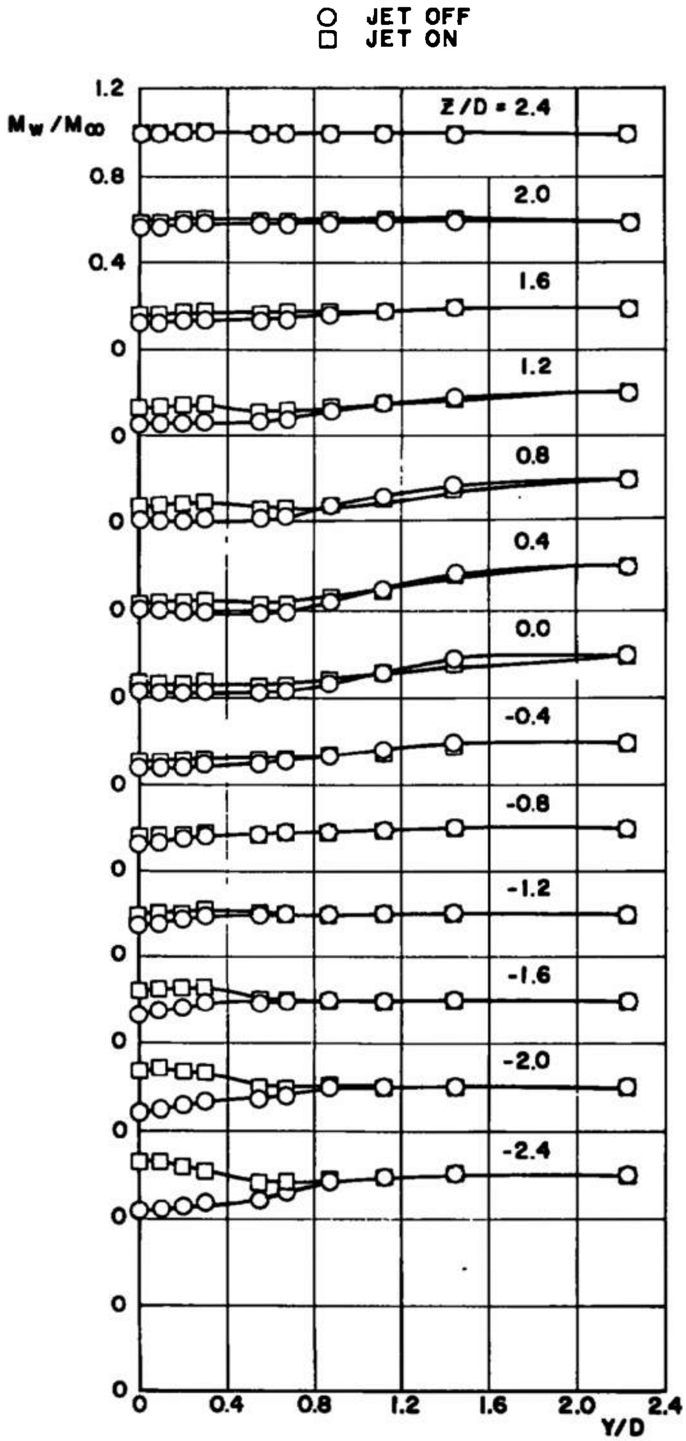

c. X/D = 9.7
Fig. 10 Concluded

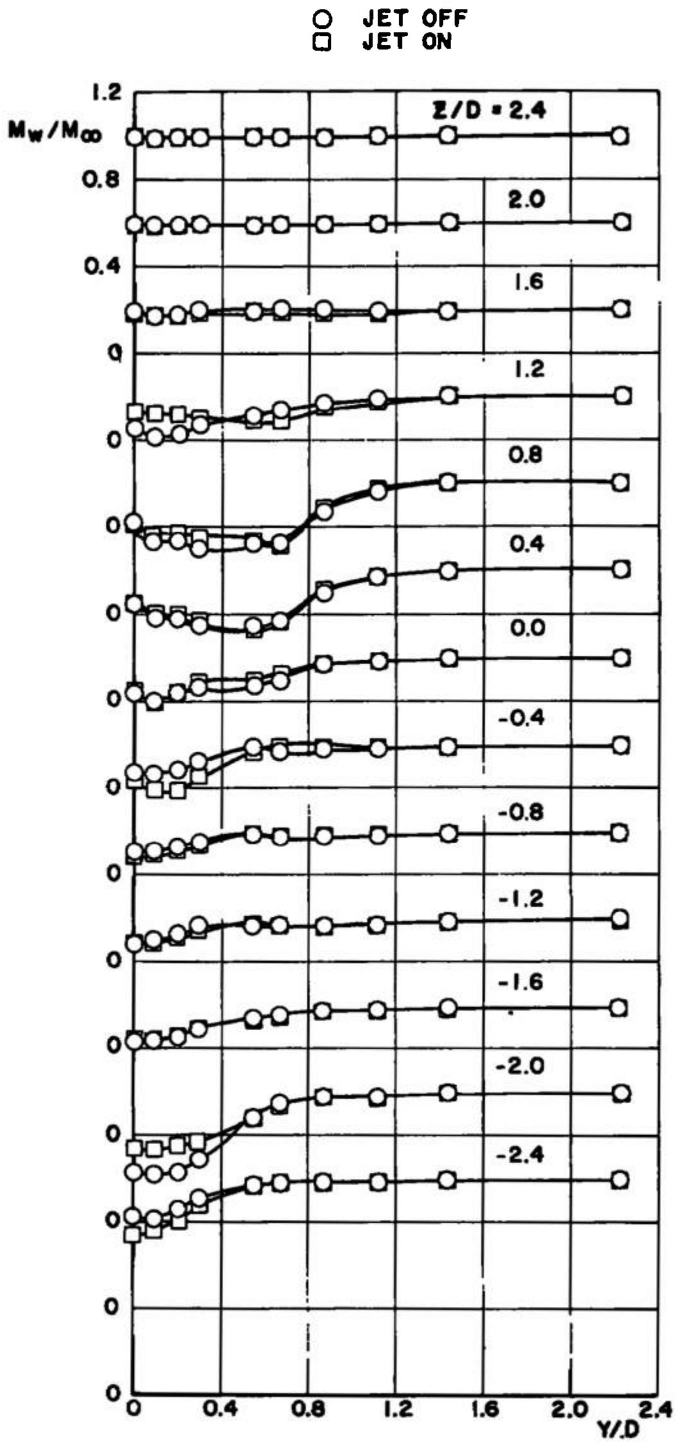

a. X/D = 5.8

Fig. 11 Local Mach Number Variation for Jet-Off and Jet-On Conditions, M_∞ = 1.50, a = 0 deg

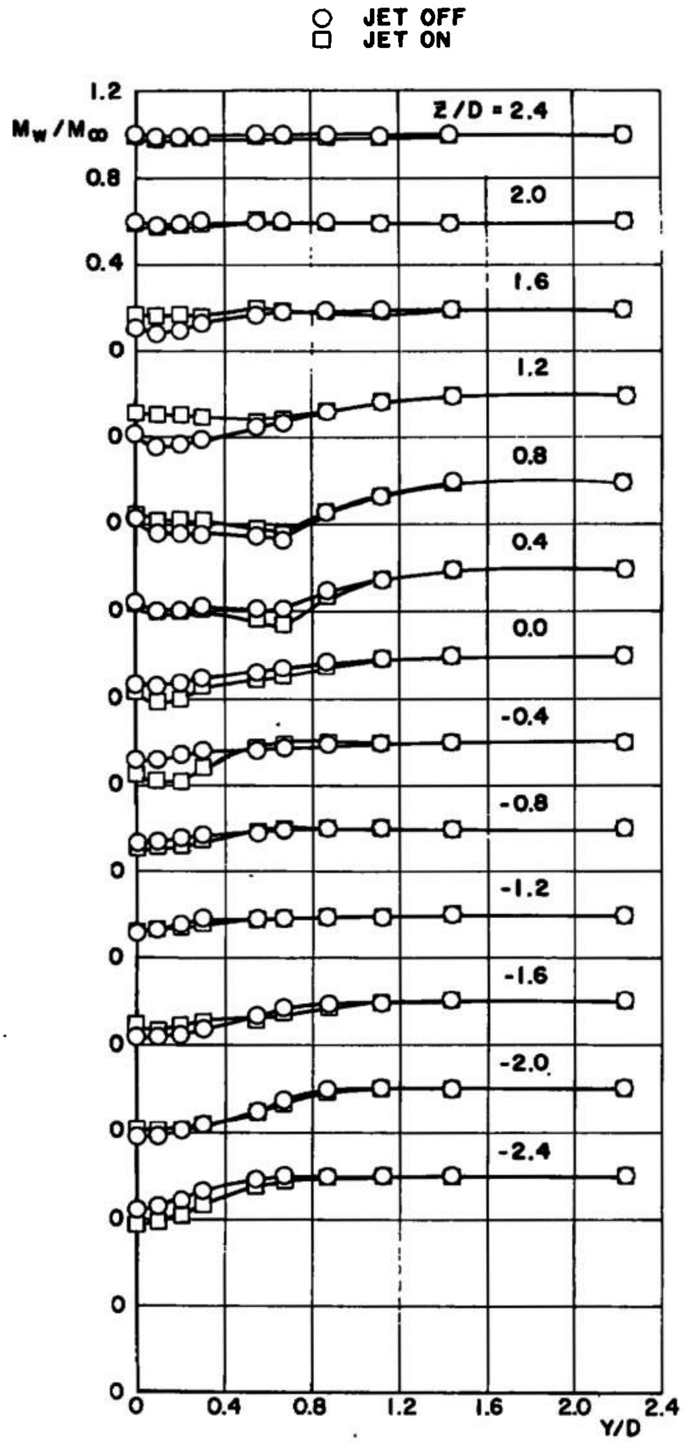

b. X/D = 7.8
Fig. 11 Continued

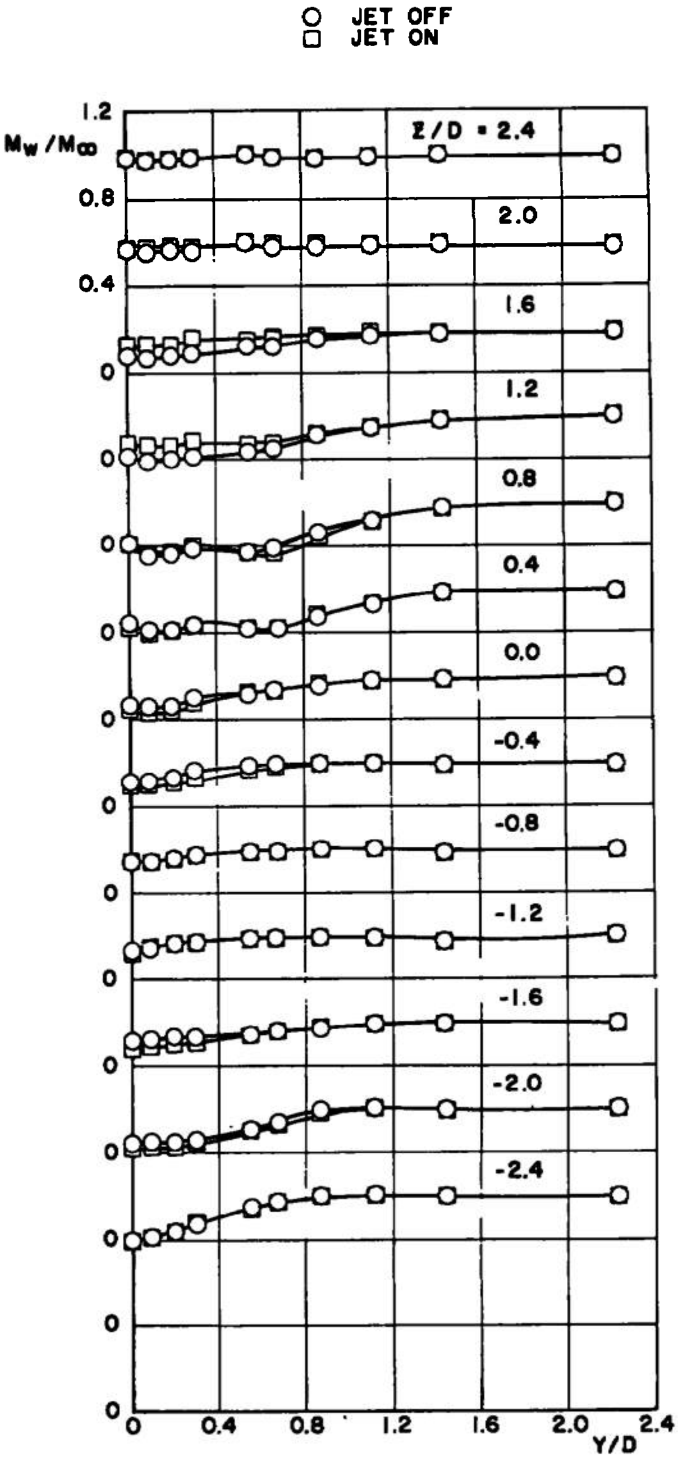

c. X/D = 9.7
Fig. 11 Concluded

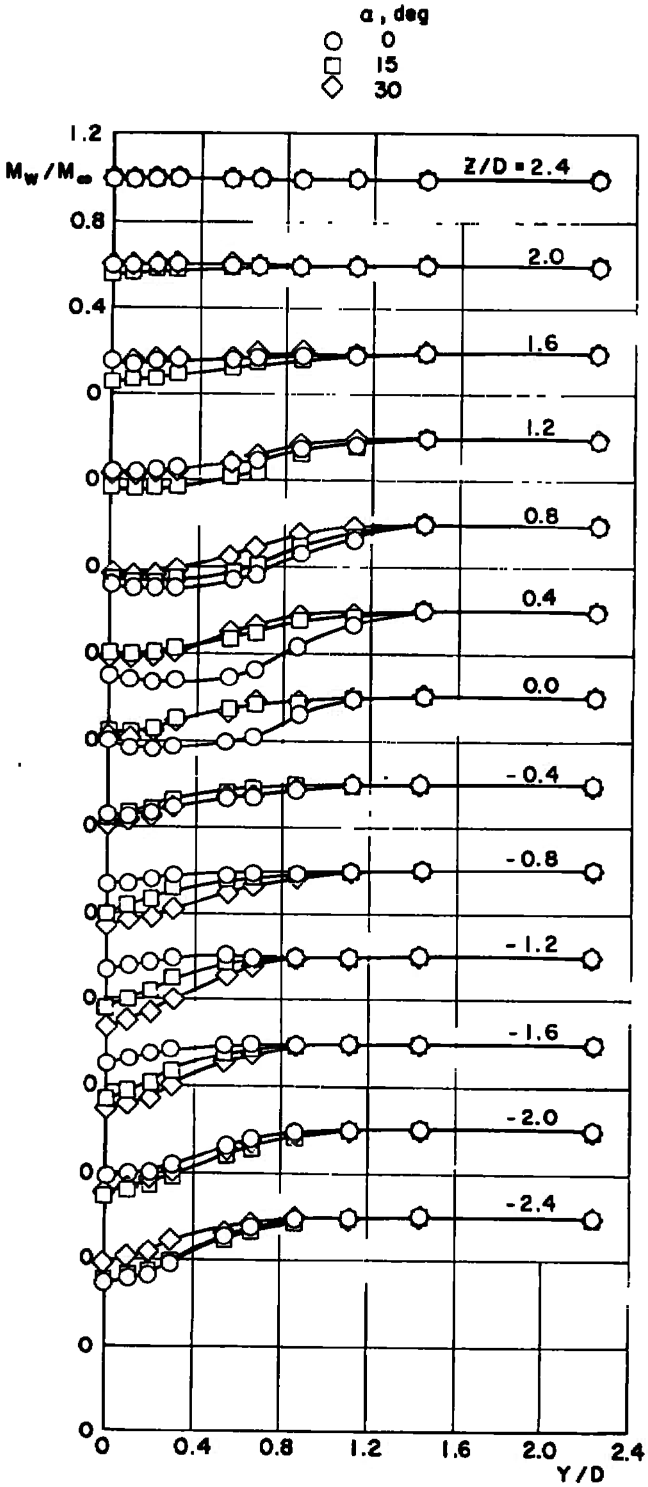

a. $M_\infty = 0.60$

Fig. 12 Variation of Local Mach Number with Model Angle of Attack, X/D = 5.8, Jet-Off

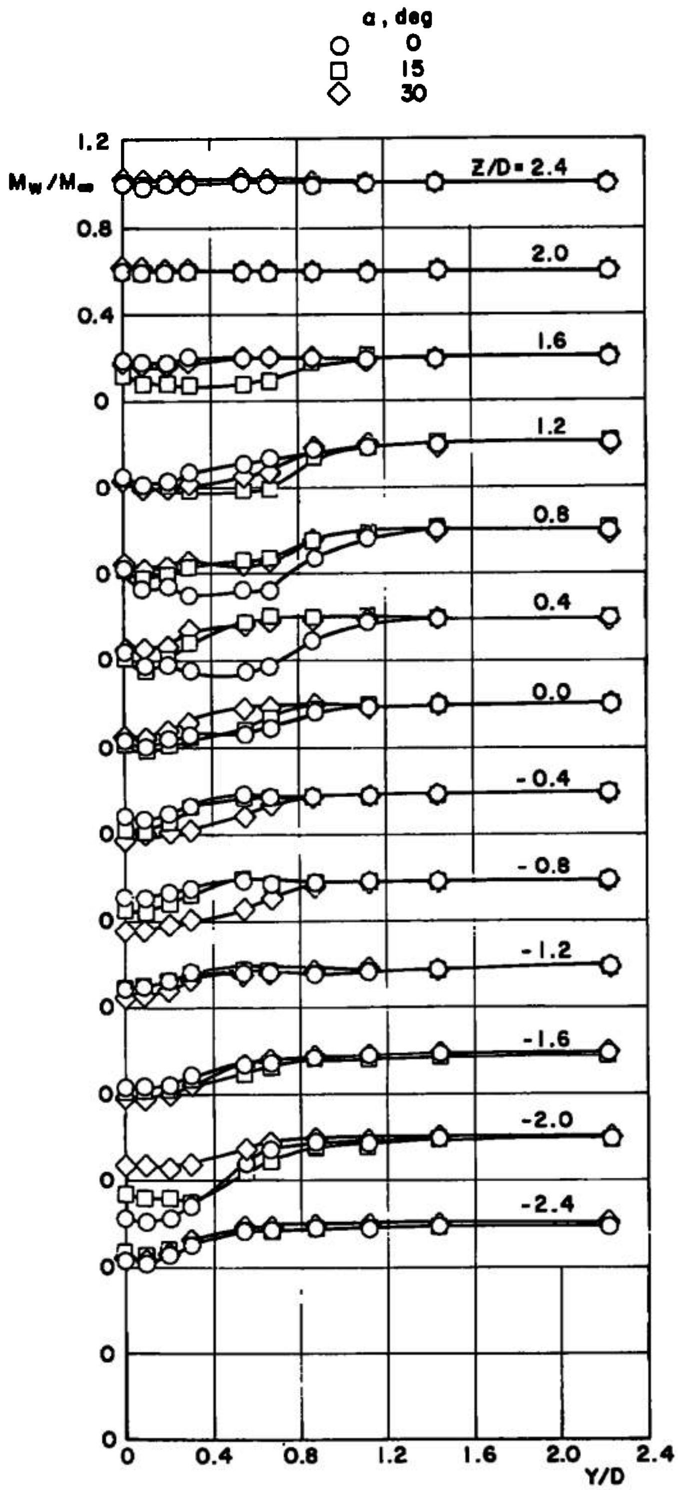

b. M_∞ = 1.50
Fig. 12 Concluded

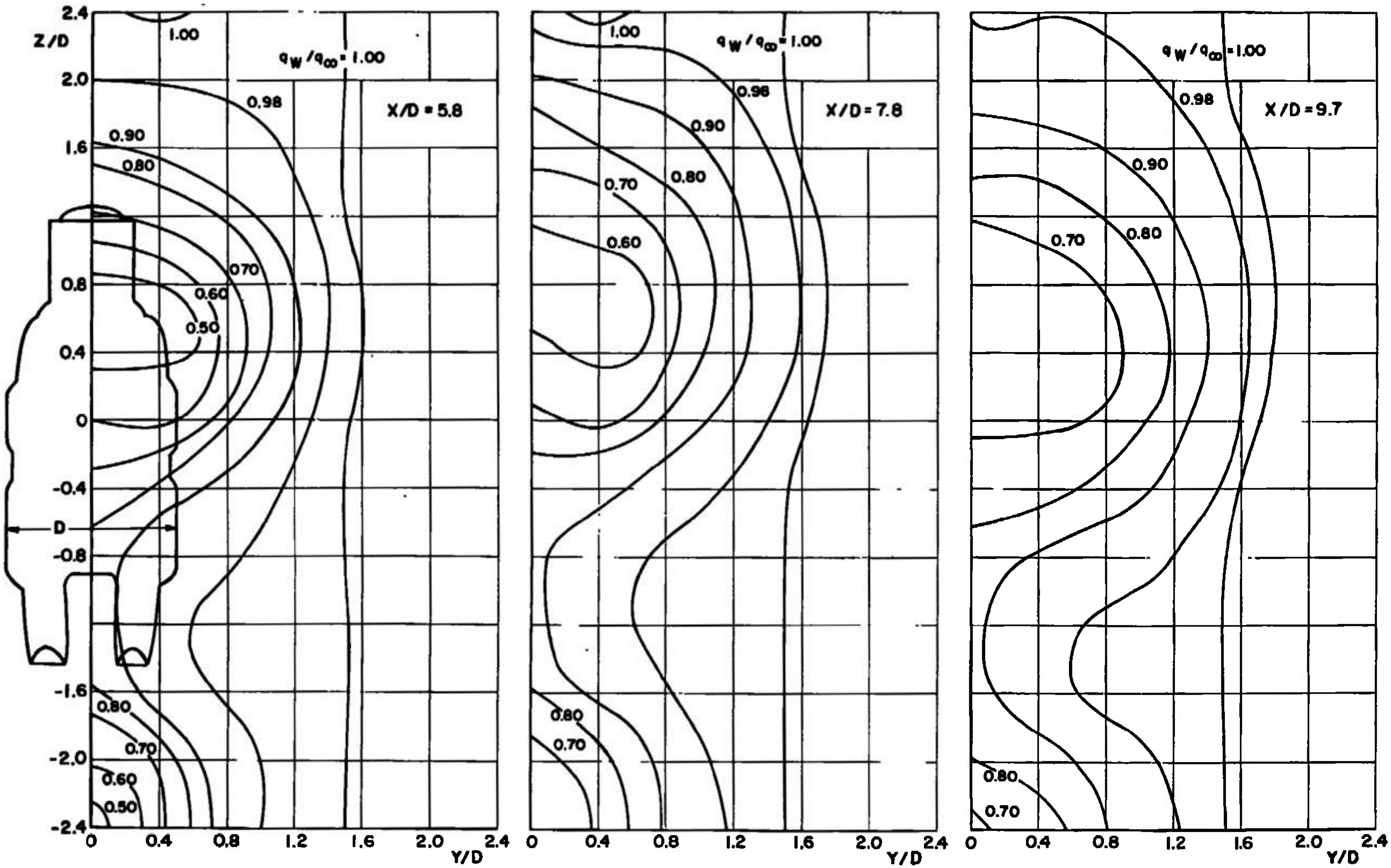

a. Jet-Off

Fig. 13 Dynamic Pressure Distribution, $M_\infty = 0.60$, $a = 0$ deg

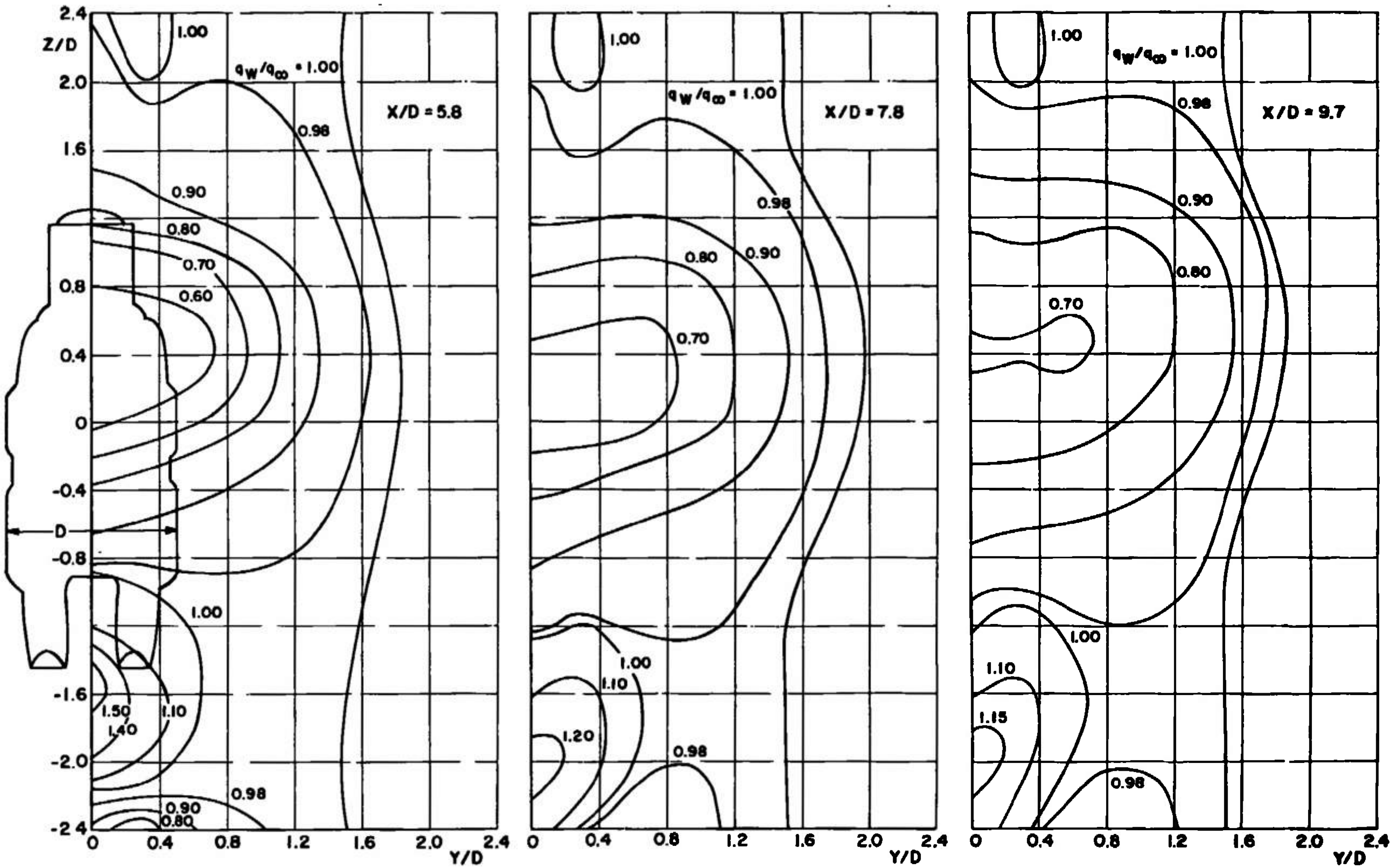

b. Jet-On
Fig. 13 Concluded

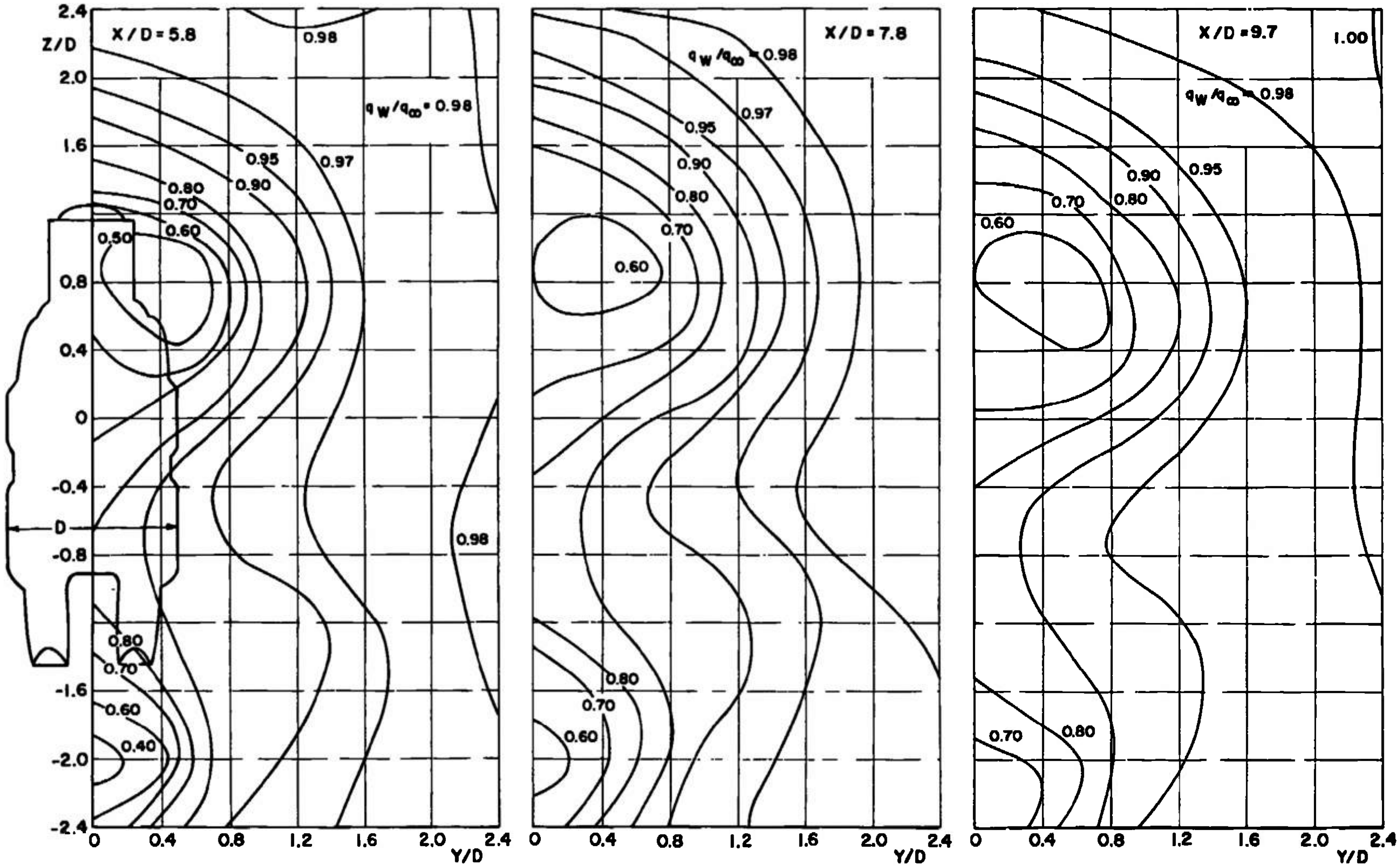

a. Jet-Off

Fig. 14 Dynamic Pressure Distribution, M_∞ = 1.50, α = 0 deg

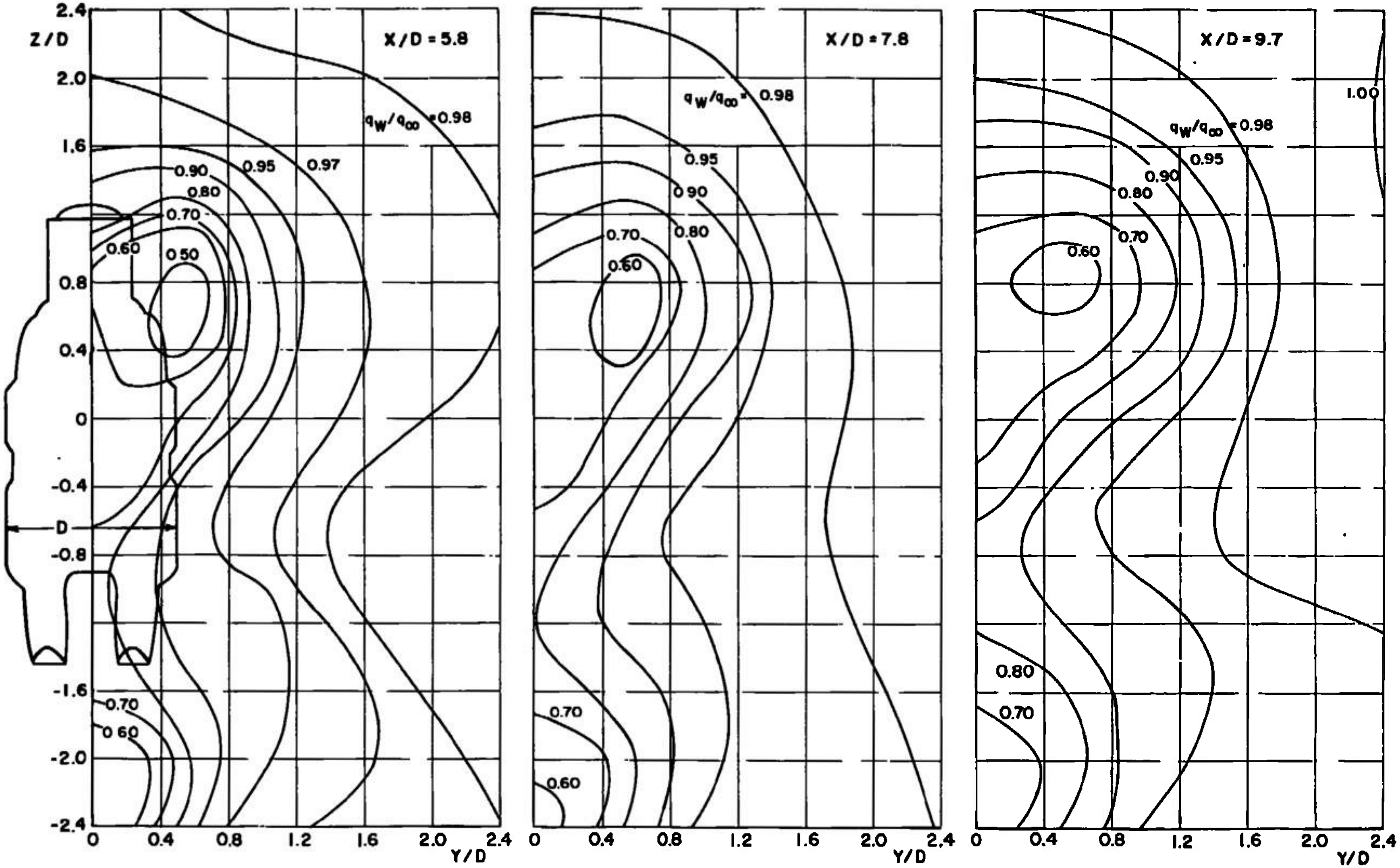

b. Jet-On
Fig. 14 Concluded

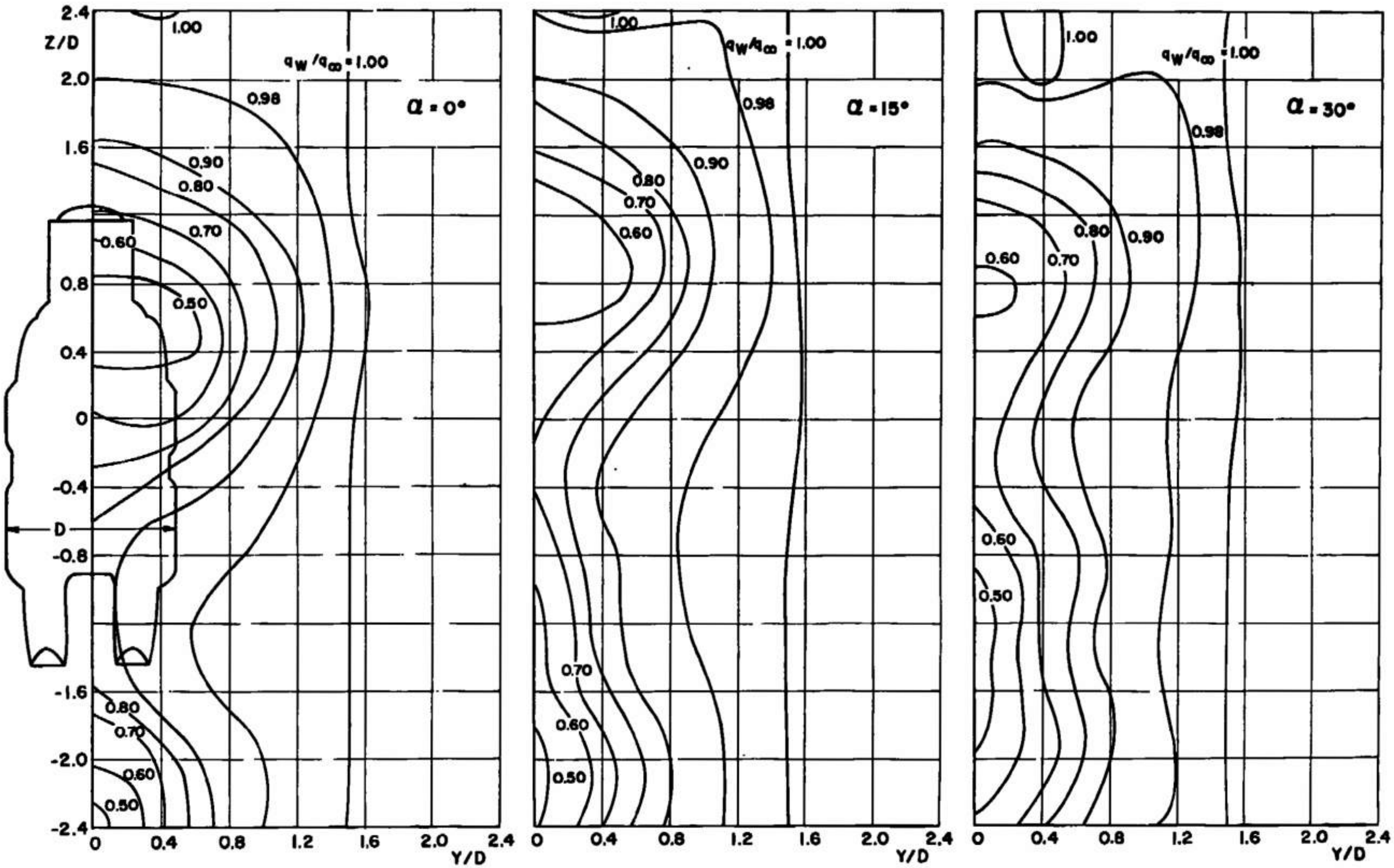

a. $M_\infty = 0.60$

Fig. 15 Variation of Local Dynamic Pressure with Model Angle of Attack, X/D = 5.8, Jet-Off

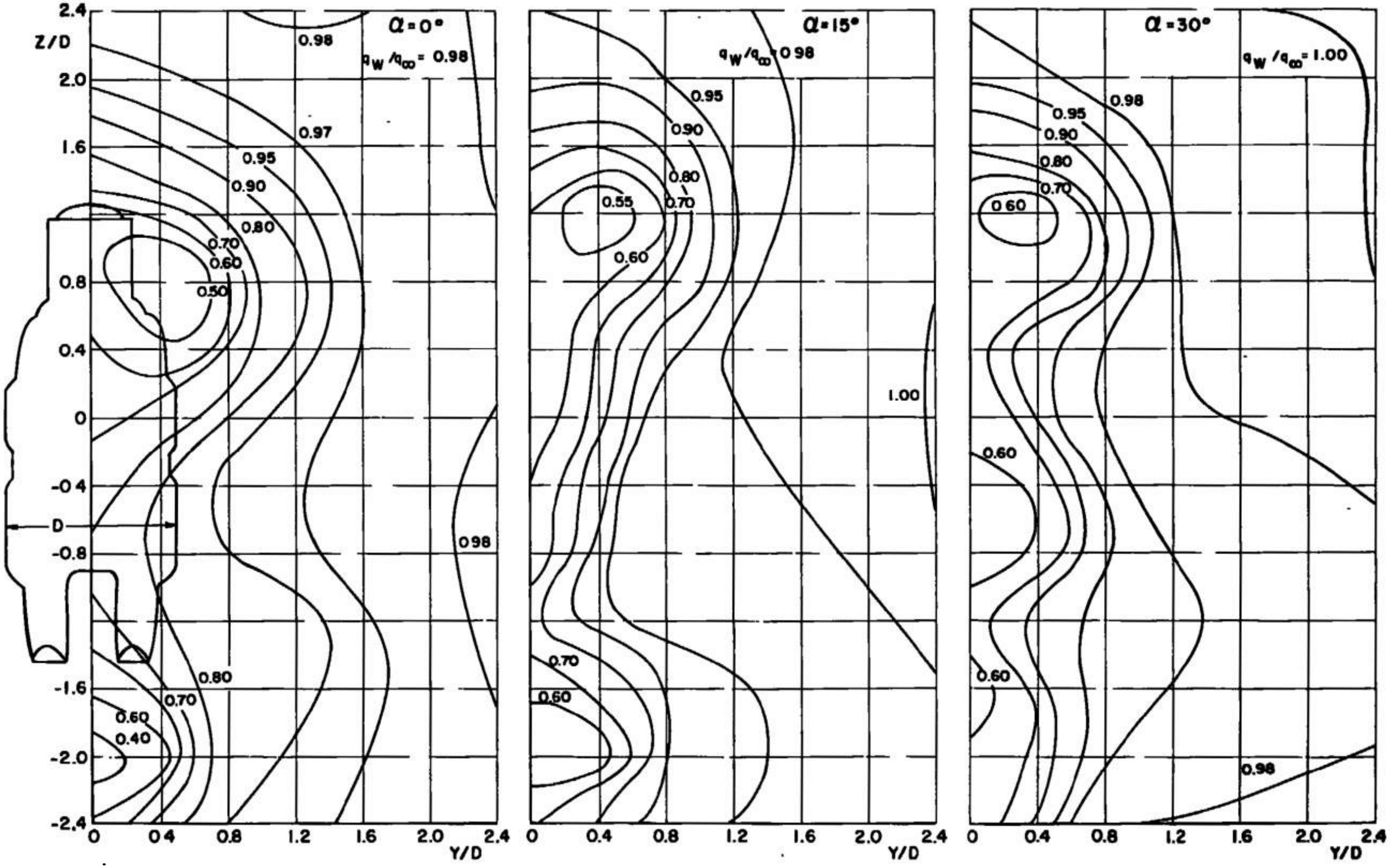

b. M_∞ = 1.50
Fig. 15 Concluded

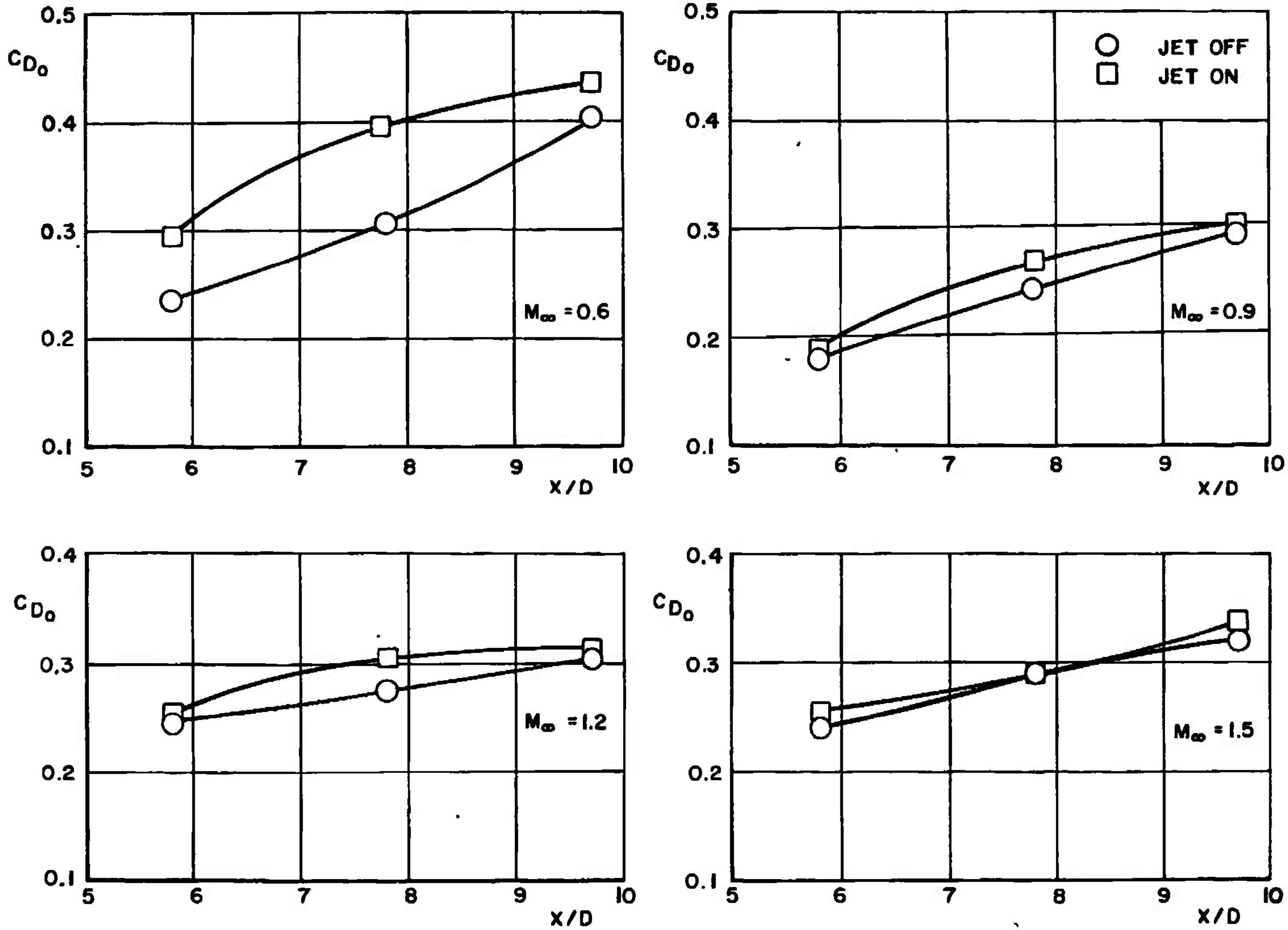

Fig. 16 Effect of Trail Distance (X/D) on the Hemisflo Drag Coefficient for Jet-Off and Jet-On Conditions at Various Mach Numbers, $\alpha = 0$ deg

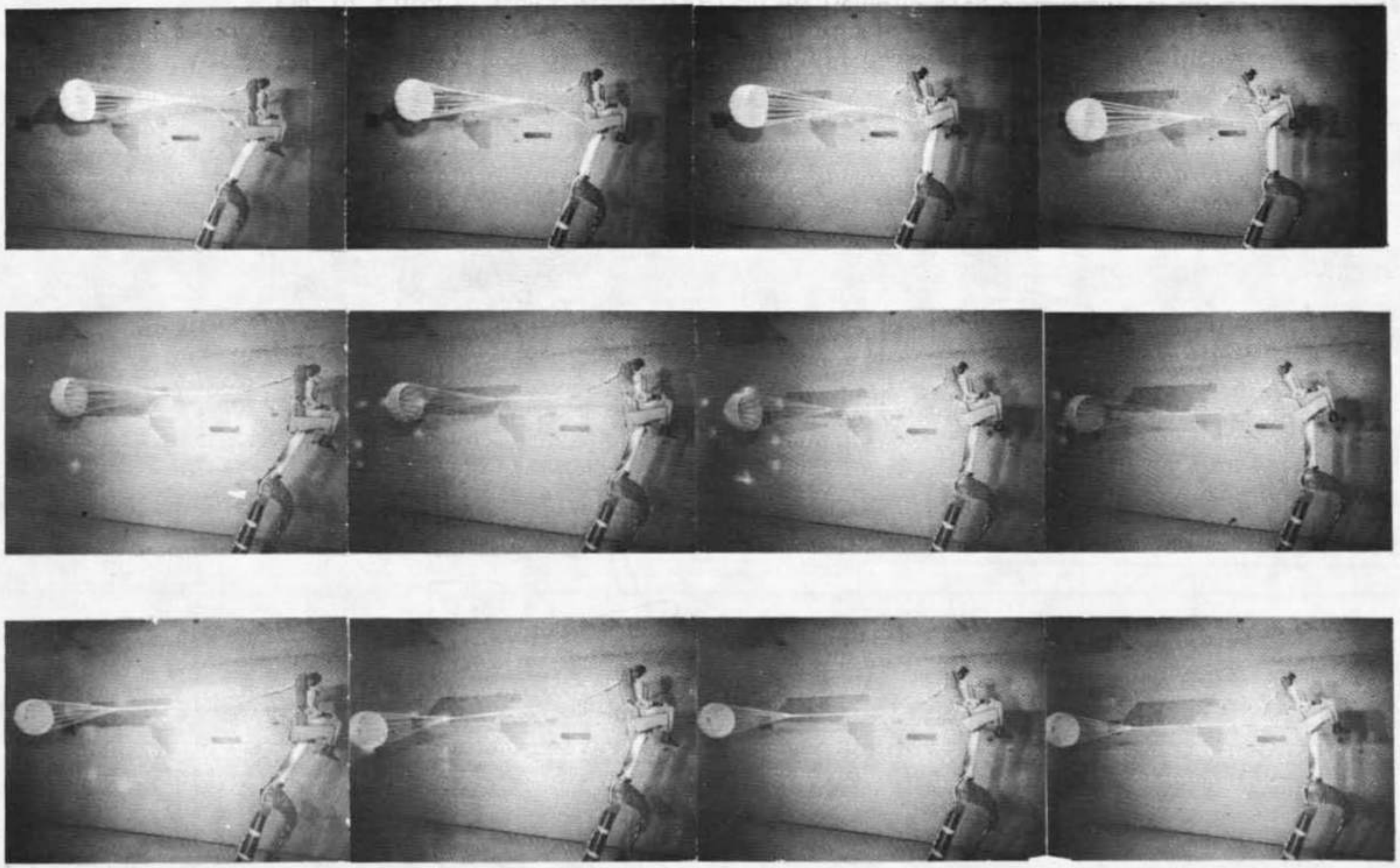

X/D

5.85

7.70

9.75

α = 0 10 deg 20 deg 30 deg

Fig. 17 Photographs of the Hemisflo Parachute at Various Trail Distances and Model Angles of Attack, $M_\infty = 0.9$, Jet-Off

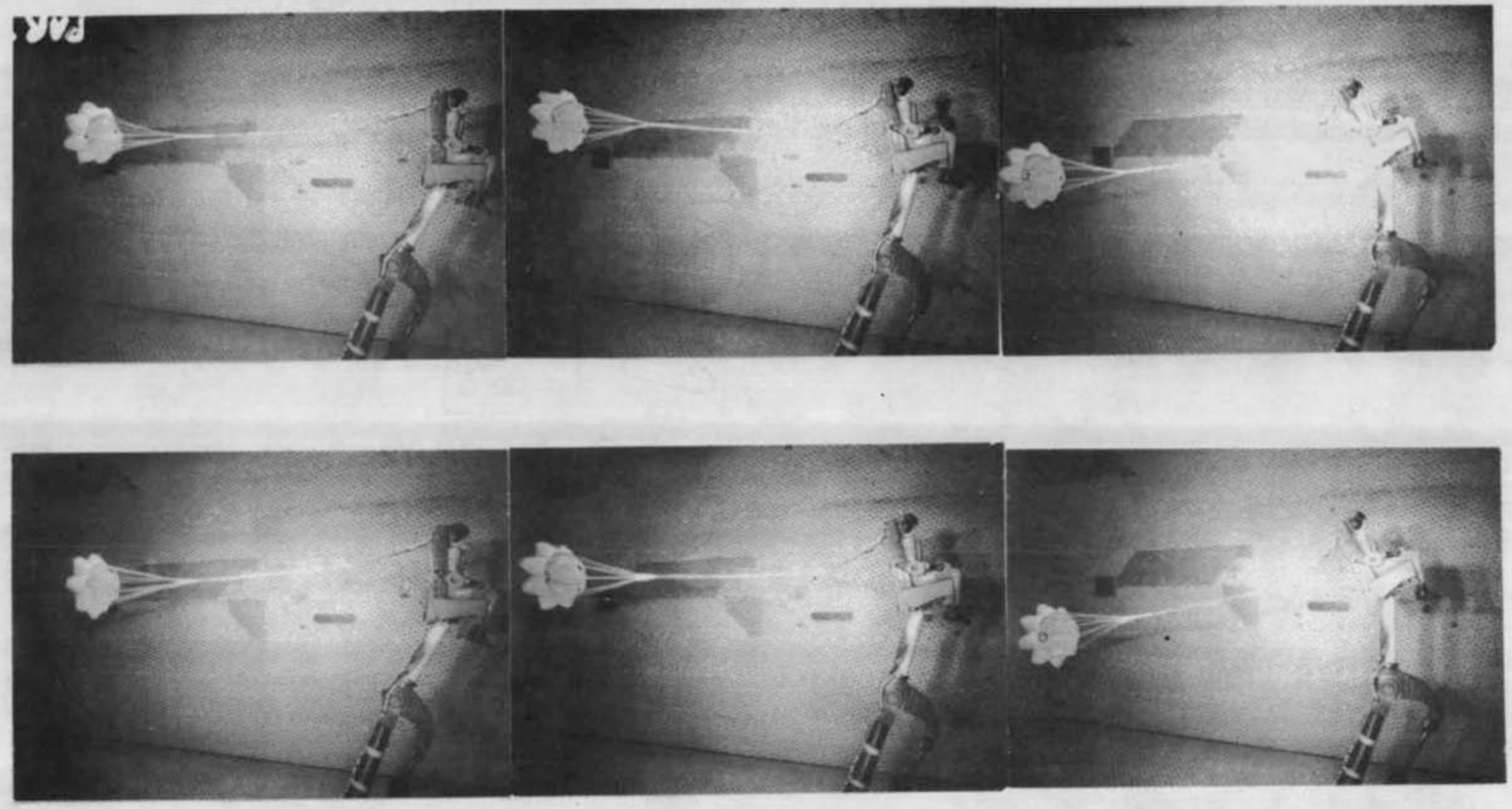

Jet Off

Jet On

$\alpha = 0$ 15 deg 30 deg

Fig. 18 Photographs of the Guide Surface Parachute at Various Model Angles of Attack Showing the Effect of Simulated Jet-On Conditions, $M_\infty = 0.9$, $X/D = 7.8$

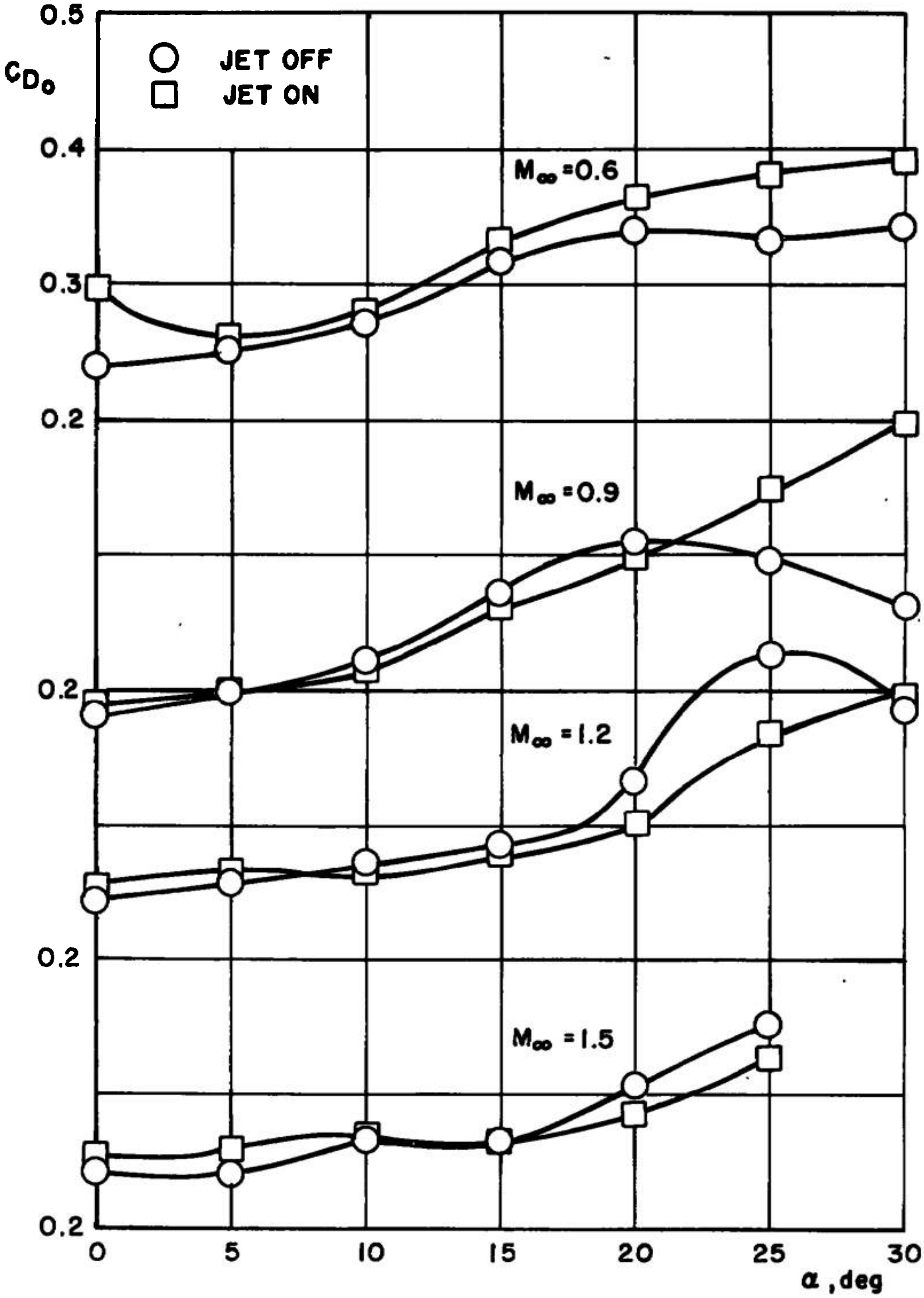

a. X/D = 5.8

Fig. 19 Effect of Model Angle of Attack on the Hemisflo Drag Coefficient at Various Trail Distances

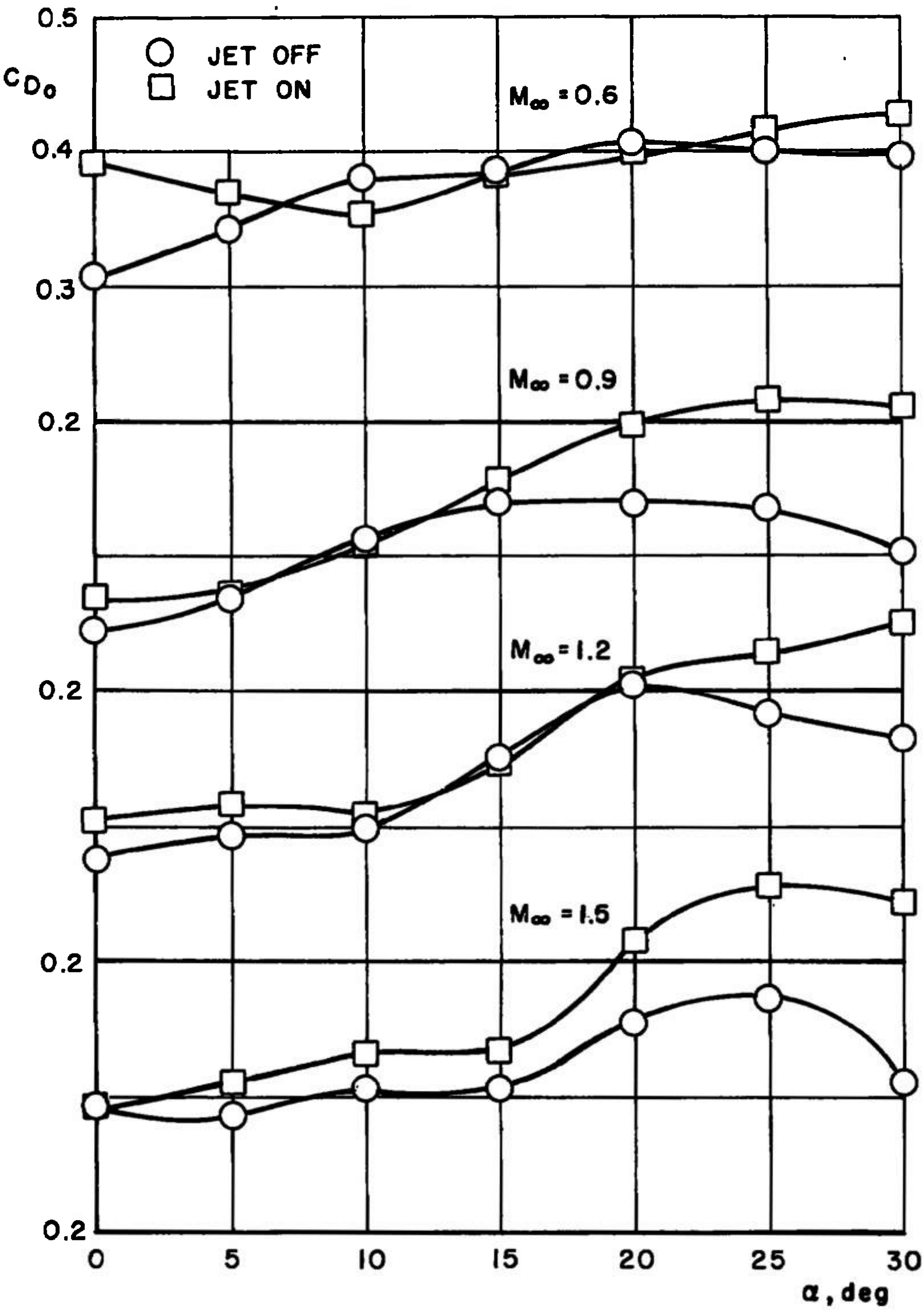

b. X/D = 7.8
Fig. 19 Continued

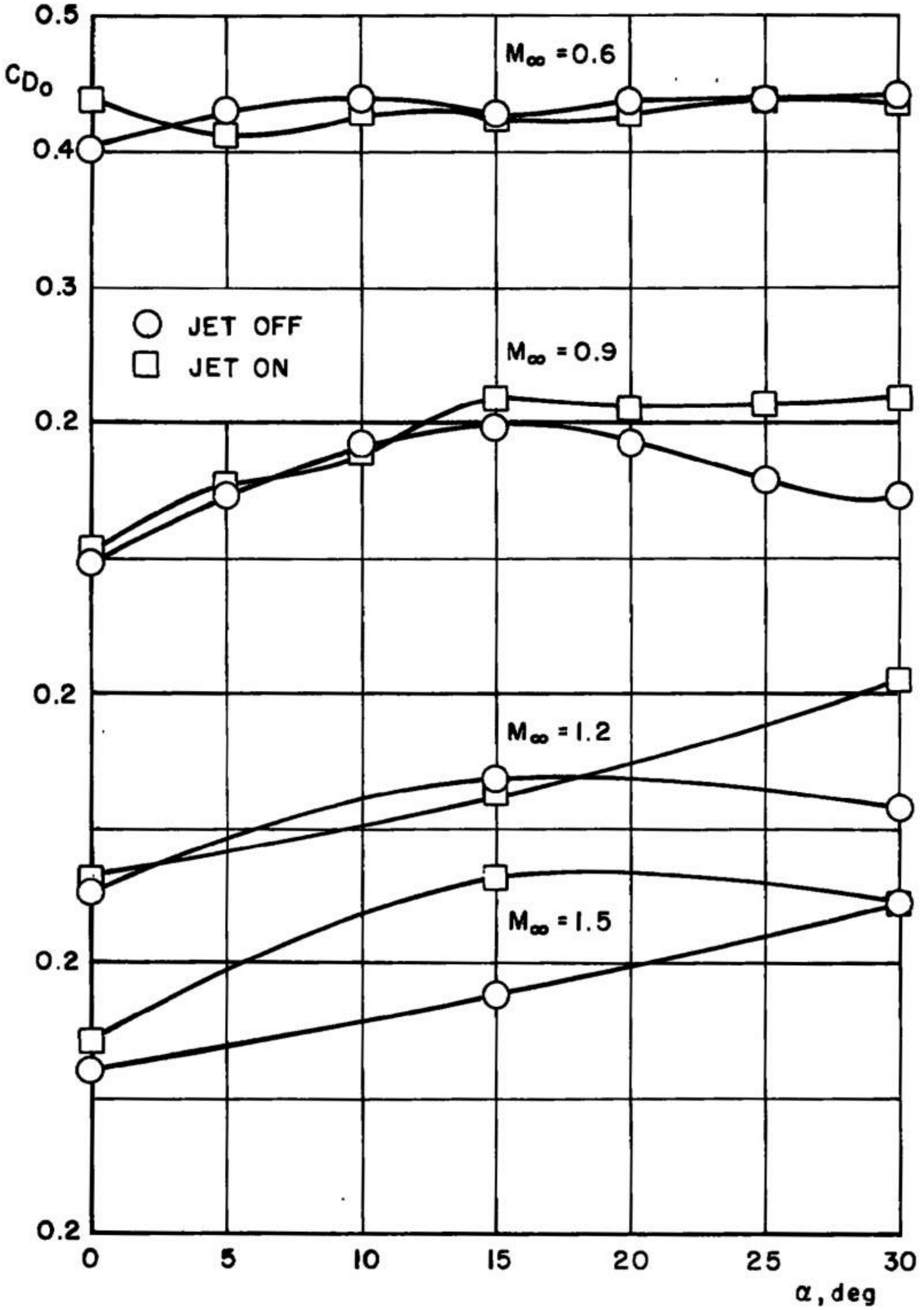

c. X/D = 9.2
Fig. 19 Concluded

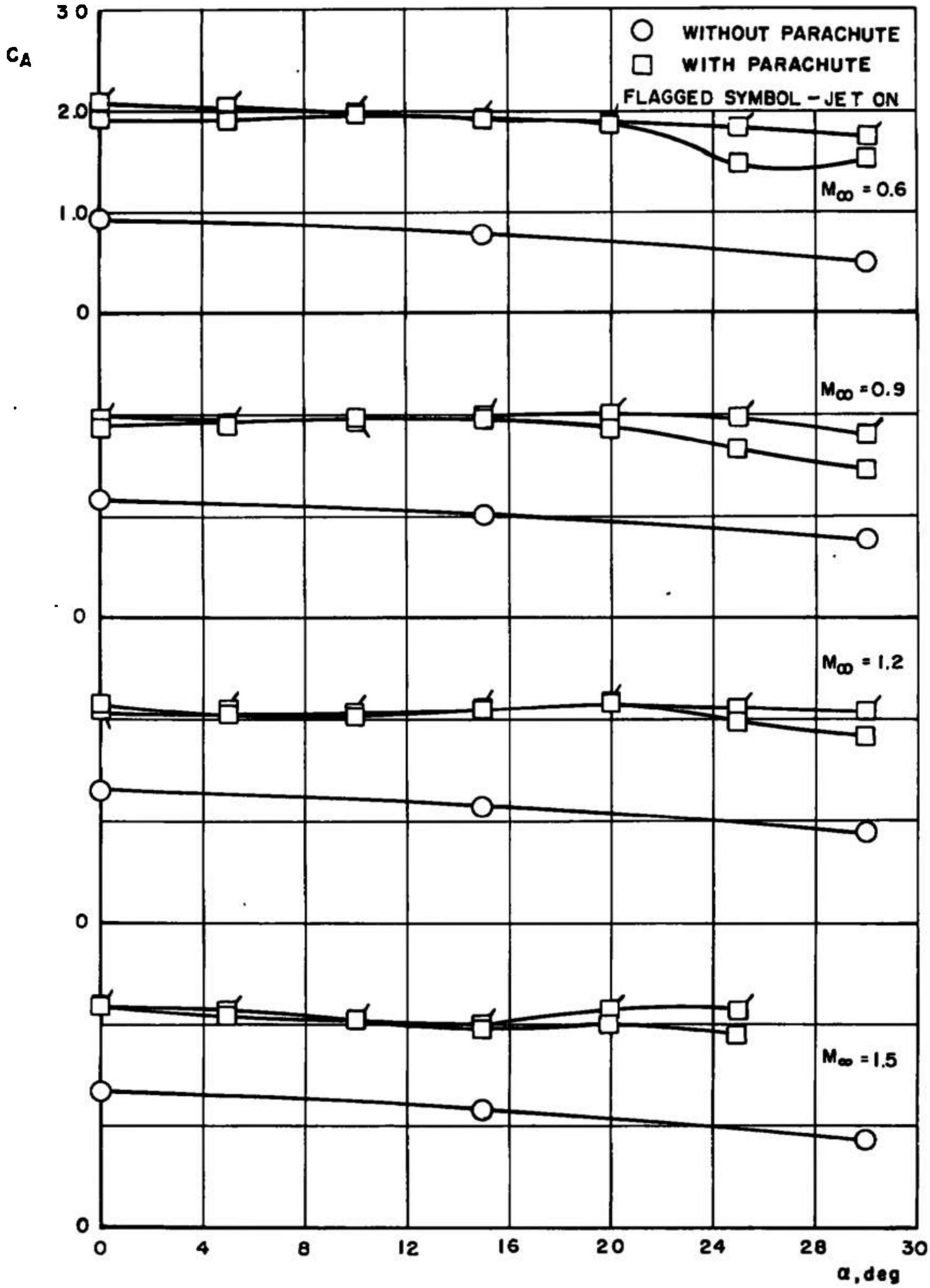

Fig. 20 Effect of Angle of Attack on the Ejection Seat Axial-Force Coefficient for Various Mach Numbers with and without a Parachute, X/D = 7.8

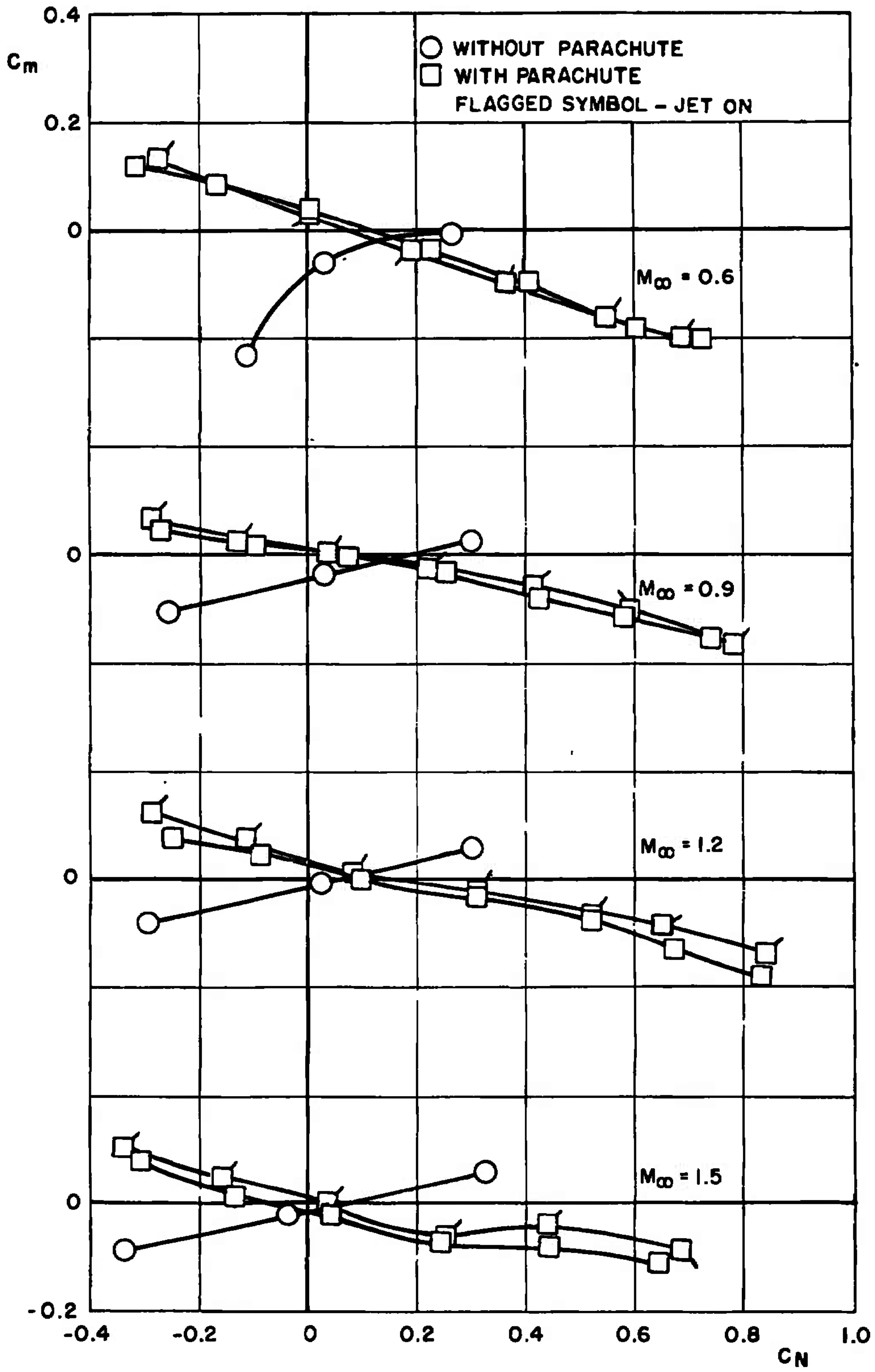

Fig. 21 Ejection Seat Pitching Moment as a Function of Normal Force with and without a Parachute, X/D = 7.8

UNCLASSIFIED

Security Classification

DOCUMENT CONTROL DATA - R & D

(Security classification of title, body of abstract and indexing annotation must be entered when the overall report is classified)

1. ORIGINATING ACTIVITY *(Corporate author)* Arnold Engineering Development Center ARO, Inc., Operating Contractor Arnold Air Force Station, Tennessee	2a. REPORT SECURITY CLASSIFICATION UNCLASSIFIED 2b. GROUP N/A

3. REPORT TITLE

WAKE PROPERTIES BEHIND AN EJECTION SEAT ESCAPE SYSTEM AND AERODYNAMIC CHARACTERISTICS WITH STABILIZATION PARACHUTES AT MACH NUMBERS FROM 0.6 TO 1.5

4. DESCRIPTIVE NOTES *(Type of report and inclusive dates)*

Final Report - September 9 to 12 and October 13 to 14, 1970

5. AUTHOR(S) *(First name, middle initial, last name)*

David E. A. Reichenau, ARO, Inc.

This document has been approved for public release its distribution is unlimited. Per AF Letter 14 Oct 74, ddc 16 Oct 74 signed William O. Cole

6. REPORT DATE February 1971	7a. TOTAL NO. OF PAGES 51	7b. NO. OF REFS 3
8a. CONTRACT OR GRANT NO F40600-71-C-0002 b. PROJECT NO 1362 c. Program Element 62201F d. Task 12	9a. ORIGINATOR'S REPORT NUMBER(S) AEDC-TR-71-30 9b. OTHER REPORT NO(S) *(Any other numbers that may be assigned this report)* ARO-PWT-TR-70-332	

10 DISTRIBUTION STATEMENT ~~This document is subject to special export controls and each transmittal to foreign governments or foreign nationals may be made only with prior approval of AFFDL (FER), Wright-Patterson AFB, Ohio 45433.~~

11 SUPPLEMENTARY NOTES Available in DDC	12. SPONSORING MILITARY ACTIVITY AFFDL (FER) Wright-Patterson AFB, Ohio 45433

13 ABSTRACT

A test was conducted in the Propulsion Wind Tunnel (16T) of the Propulsion Wind Tunnel Facility to determine the flow field in the wake of an ejection seat escape system at transonic flight conditions, and to determine the performance characteristics of a stabilization parachute attached to the back of the ejection seat model. The results were obtained for both simulated rocket-off and rocket-on conditions through a model angle-of-attack range from 0 to 30 deg. High pressure air was used to simulate the escape rocket jet plume at a sea-level altitude. The results show that the ejection seat model was statically unstable, but became longitudinally stable with the parachute for the test range investigated.

~~This document is subject to special export controls and each transmittal to foreign governments or foreign nationals may be made only with prior approval of AFFDL (FER), Wright-Patterson AFB, Ohio 45433.~~

DD FORM 1 NOV 65 1473

UNCLASSIFIED

Security Classification

14. KEY WORDS	LINK A		LINK B		LINK C	
	ROLE	WT	ROLE	WT	ROLE	WT
1 ejection seats						
2 escape systems						
aerodynamic characteristics						
3 parachutes						
scale models						

AFSC
Arnold AFS Tenn